Record 2001/31

Quaternary sediment cores from the Southern Fairway Basin on the northern Lord Howe Rise

(Tasman Sea)

Gerald Dickens, Neville Exon, David Holdway, Yves Lafoy, Jean-Marie Auzende, Gavin Dunbar, and Roger Summons.

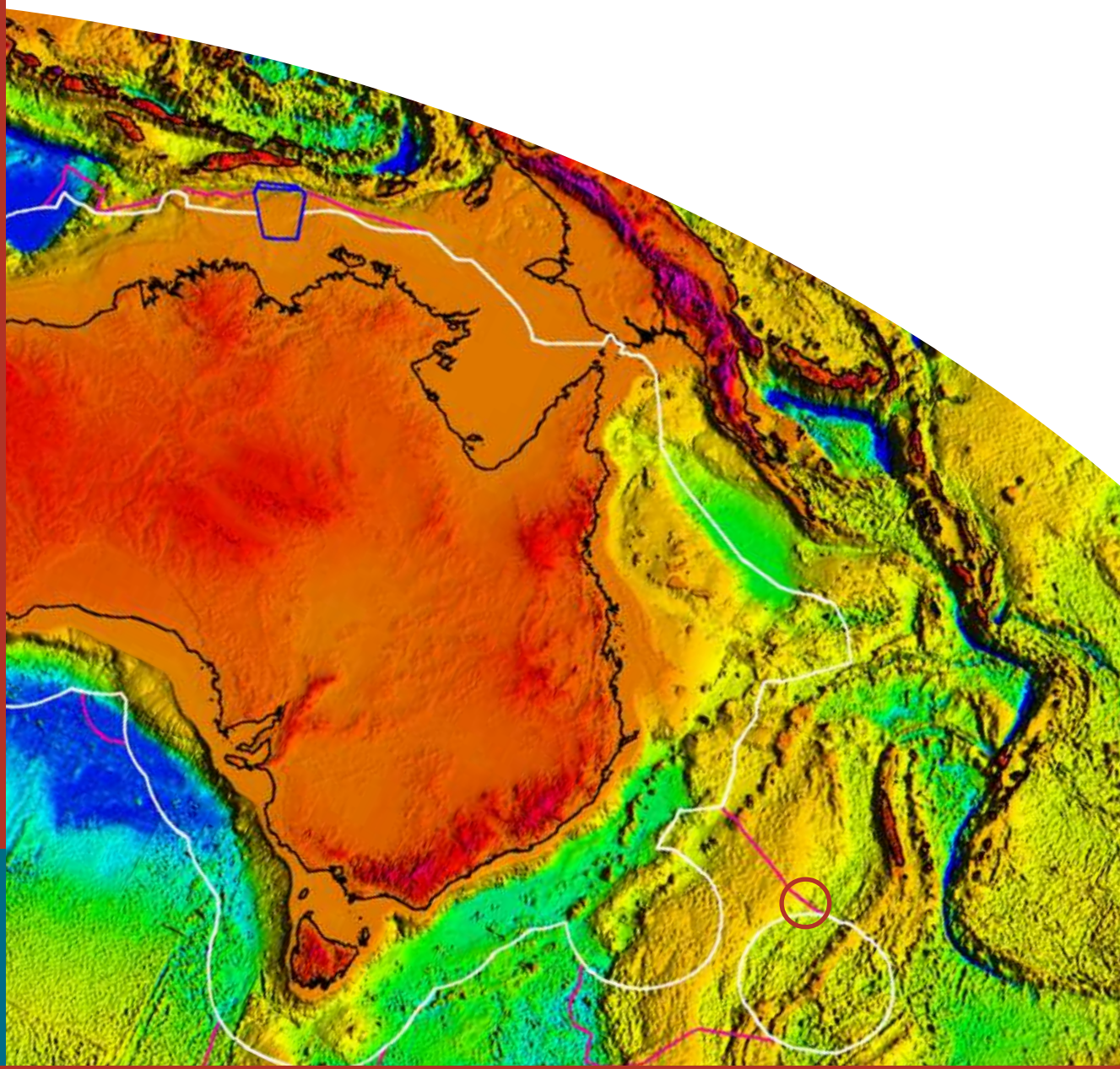

AGSO

AGSO
GEOSCIENCE
AUSTRALIA

Quaternary sediment cores from the Southern Fairway Basin on the northern Lord Howe Rise (Tasman Sea)

Gerald Dickens[1,2], Neville Exon[3], David Holdway[3], Yves Lafoy[4], Jean-Marie Auzende[5], Gavin Dunbar[1,6], and Roger Summons[3,7]

AGSO Record 2001/31

[1]School of Earth Sciences, James Cook University, Townsville, QLD 4811, Australia
[2]Department of Earth Sciences, Rice University, Houston, TX 77005-1892, USA
[3]AGSO - Geoscience Australia, Canberra, ACT 2601, Australia
[4]Service des Mines et de l'Energie, BP 465, Nouméa, Nouvelle-Calédonie
[5]IFREMER and Delegate for Research and Technology, BP C5, Nouméa, Nouvelle-Calédonie
[6]Antarctic Research Centre, Victoria University, Wellington, New Zealand
[7]Department of Earth, Atmospheric and Planetary Sciences, Massachusetts Institute of Technology, 77 Massachusetts Avenue, Cambridge 02139, USA

AGSO – Geoscience Australia

Chief Executive Officer: Neil Williams

Department of Industry, Science & Resources

Minister for Industry, Science & Resources: Senator The Hon. Nick Minchin
Parliamentary Secretary: The Hon. Warren Entsch, MP

ISSN: 1039-0073
ISBN: 0 642 467110

Bibliographic reference: Dickens G., Exon N., Holdway D., Lafoy Y., Auzende J.M., Dunbar G., Summons R., 2001. *Quaternary sediment cores from the Southern Fairway Basin on the northern Lord Howe Rise (Tasman Sea).* AGSO – Geoscience Australia, Record 2001/31.

Contents Page

Figures

Tables

Plates 1-13 (at back). Colour photographs of the thirteen *ZoNéCo 5* cores with records of greyscale and magnetic susceptibility (MS). Shipboard colour intervals and shore-based physical property intervals (PI-PIII) also are noted.

1. ABSTRACT

Thick packages of Cretaceous and Tertiary sediment with numerous diapirs fill the Southern Fairway Basin (SFB) on the Lord Howe Rise (LHR). A bottom-simulating reflector (BSR) also extends across much of this basin, perhaps indicating substantial amounts of CH_4 as gas hydrate and free gas. As part of the *ZoNéCo 5* survey, run on behalf of the New Caledonian government, 13 piston cores were taken by the RV *L'Atalante* in 1999 to assess the gas and petroleum potential of the SFB. Specifically, the cores were recovered to document the nature of sediment, pore water and gas in the shallow sedimentary section.

The 13 cores, from 1250 to 2753 m below sea level (mbsl) and between 405 and 758 cm long, contain stiff nannofossil ooze. If average regional sedimentation rates apply (10 m/my), the maximum age at the bottom of cores is less than 800,000 years. The sediment typically grades from greyish orange at the top, to very pale orange in the middle, and then to either yellowish grey, very light grey or white at the bottom. Thin black horizons, presumably composed of pyrite, also occur. The changes in colour are related to variations in magnetic susceptibility (MS) and pore water SO_4^{2-}. Pale and grey zones generally have low MS punctuated by MS highs, and low pore water SO_4^{2-} concentrations. Methane was detected in most sediment samples, although at trace levels. The presence of ethane, propane and higher hydrocarbons suggests that gases in the SFB have a thermogenic component.

With the available data, the best explanation for colour, MS and SO_4^{2-} profiles is that Fe has been remobilised under anoxic conditions. Ferric iron in solid oxyhydroxide phases and SO_4^{2-} in pore waters have been converted to dissolved ferrous iron and sulphide. Some of this iron and sulphur has then re-precipitated as pyrite or magnetite (the MS spikes). The overall process may be driven by CH_4 from underlying gas hydrate deposits. Upward fluxes of CH_4, perhaps of thermogenic origin, induce anaerobic CH_4 oxidation in shallow sediment, a process that consumes SO_4^{2-}. As a consequence, unexpectedly shallow redox fronts occur in the SFB. However, longer cores with less-oxidised sediment and additional analyses are needed to understand sediment, water and gas in this region.

Key words: marine sediment cores, redox fronts, gas hydrate, diapirs, ZoNéCo 5 survey, L'Atalante, Lord Howe Rise, Fairway Basin.

2. INTRODUCTION

From October 14 to November 7, 1999, the *ZoNéCo 5* cruise of IFREMER's RV *L'Atalante* investigated a potential frontier petroleum province on the northern Lord Howe Rise (LHR), a region immediately north of the agreed seabed boundary between Australia and France (**Fig. 1**). This report covers the coring program of the cruise.

With crestal water depths between 750 and 1200 m below sea level (mbsl), and stretching about 1600 km in a north-south direction, the LHR is a largely unexplored bathymetric high in the Tasman Sea between Australia, New Caledonia and New Zealand (**Fig. 1**). The geology of this rise is complex and poorly understood. In general, the LHR is a thinned fragment of continental crust that detached from Gondwana during Mesozoic rifting and subsequently subsided to present depths in the early Cenozoic (e.g., Hayes & Ringis, 1973; Gaina *et al*., 1998).

Recent geophysical cruises in the northern Tasman Sea have discovered a large (> 70,000 km^2) north-south structural basin on the eastern flank of the northern LHR (Exon *et al*., 1998; Lafoy *et al*., 1998a, b; Van de Beuque *et al*., 1998; Auzende *et al*., 2000a,b). This basin (**Fig. 1**), probably the southern extension of the Fairway Basin (SFB) and hereafter referred to as such,

contains several kilometres of sediment and three very interesting phenomena (Exon *et al*., 1998; Auzende *et al*., 2000a, b): a bottom simulating reflector (BSR), numerous diapirs, and an unusually rough seafloor topography. Radarsat analyses (arranged by Dr Geoff O'Brien at AGSO in 1999) also show some anomalies on the sea surface above the SFB, which were regarded as natural films or possible seepage slicks.

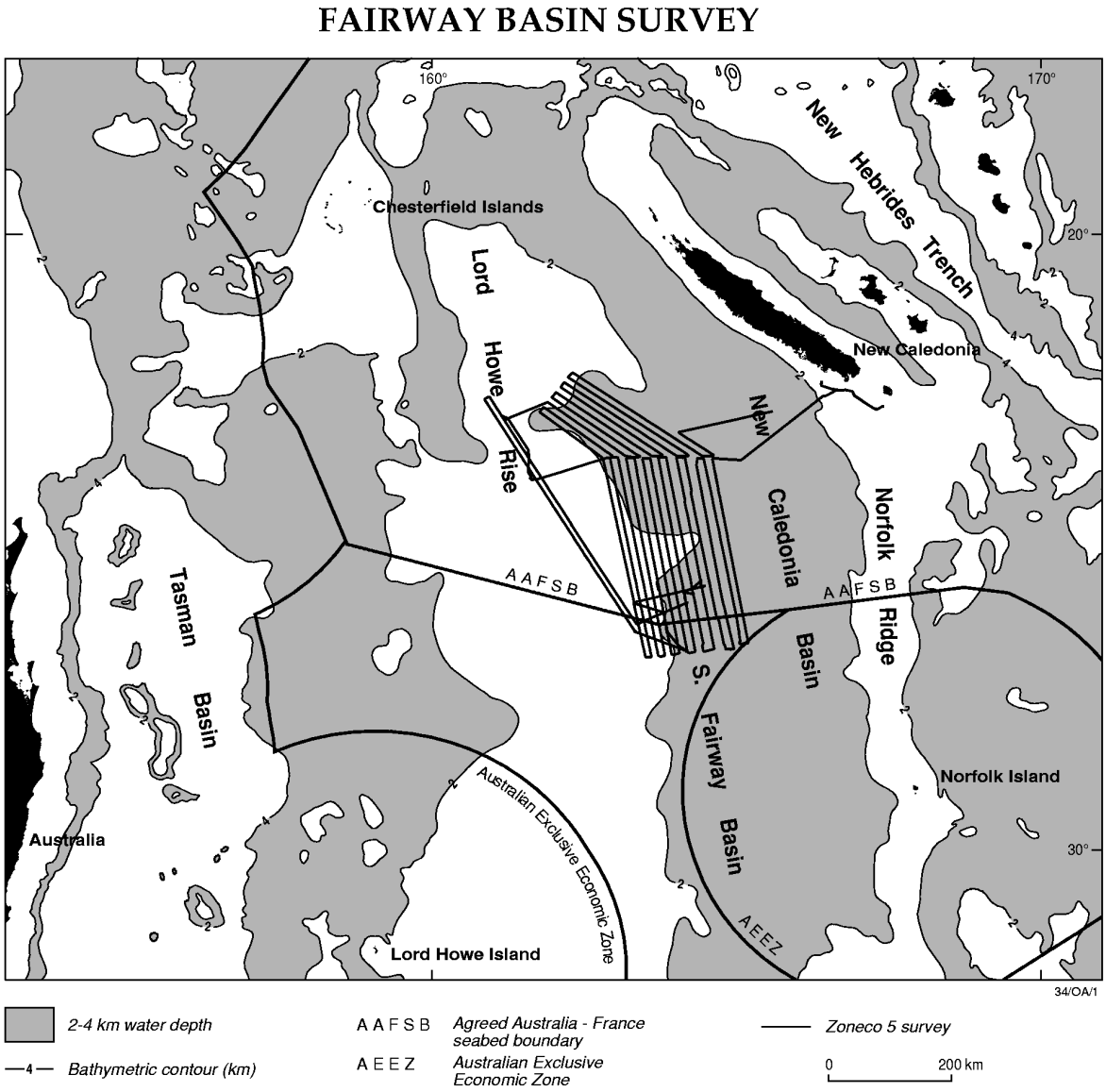

Figure 1. Map of the Tasman Sea showing the Lord Howe Rise (LHR), the Southern Fairway Basin (SFB), and regions of Australian and French jurisdiction. The area covered by the ZoNéCo 5 survey is indicated by the track lines.

The BSR of the SFB is a prominent reflector on seismic profiles that cuts across lithology at 0.65 to 0.75s two-way travel time (twt) below the seafloor (**Figs. 2, 3, 4**).Using the best estimates for sonic velocity (1600 m/s) and thermal gradients (0.9 + 0.04°C/m) in sediment on the LHR (Morin, 1986; Morin & von Herzen, 1986), predicted pressures and temperatures at the depth of the BSR lie on the CH_4-CH_4 hydrate-seawater equilibrium curve (Dickens & Quinby-Hunt,1994)

In other areas, BSRs at these conditions mark an interface between overlying gas hydrate and underlying free gas (e.g., Bangs *et al*., 1993; MacKay *et al*., 1994; Dickens *et al*., 1997). The BSR of the SFB may also represent a gas hydrate-free gas interface (Exon *et al*., 1998).

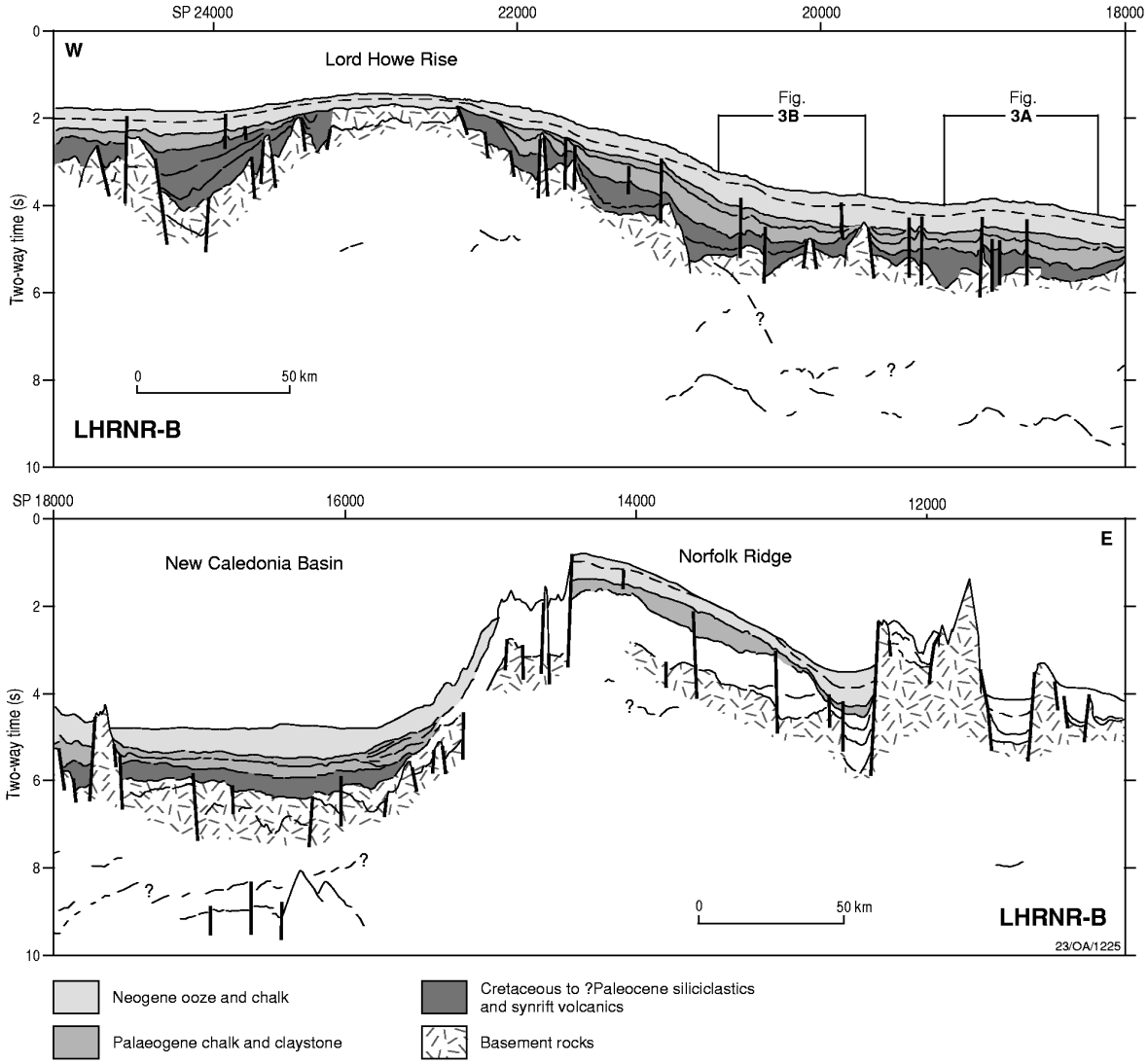

Figure 2. Line drawing of seismic profile AGSO177/LHRNR-B from a RV *Rig Seismic* cruise across the Southern Fairway Basin (SFB) near the French-Australian seabed boundary (**Fig. 1**). Note that the SFB consists of a series of faulted basement blocks overlain by thick Cretaceous and Palaeogene sediment sequences (from Exon *et al*., 1998).

At least 100 diapirs with a diameter of 5 to 15 km have been identified on seismic profiles across the SFB (Auzende *et al*., 2000a, b). These diapirs are sourced from a homogeneous sediment layer at about 2.0 to 2.5 s twt below the seafloor, and rise vertically through the overlying sediment, often to within 0.5 s twt of the seafloor (**Fig. 4**). Salt and mud diapirs are common phenomena in thick sediment sequences of rift basins (e.g., Pautot *et al*., 1970; Auzende *et al*., 1971). The diapirs in the SFB are probably composed of salt or mud that originally was deposited during the early stages of Cretaceous rifting (Auzende *et al*., 2000a).

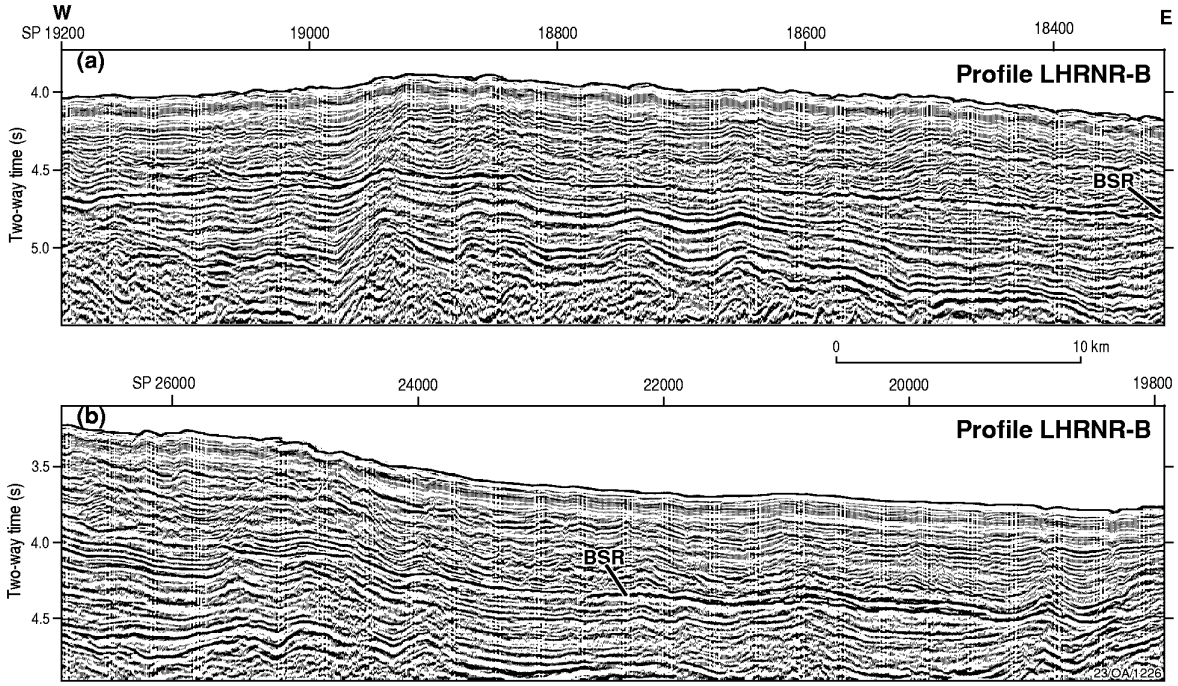

Figure 3. Detailed sections of seismic profile AGSO177/LHRNR-B (**Fig. 2**) showing the Bottom Simulating Reflector (BSR) in the SFB (from Exon *et al.*, 1998).

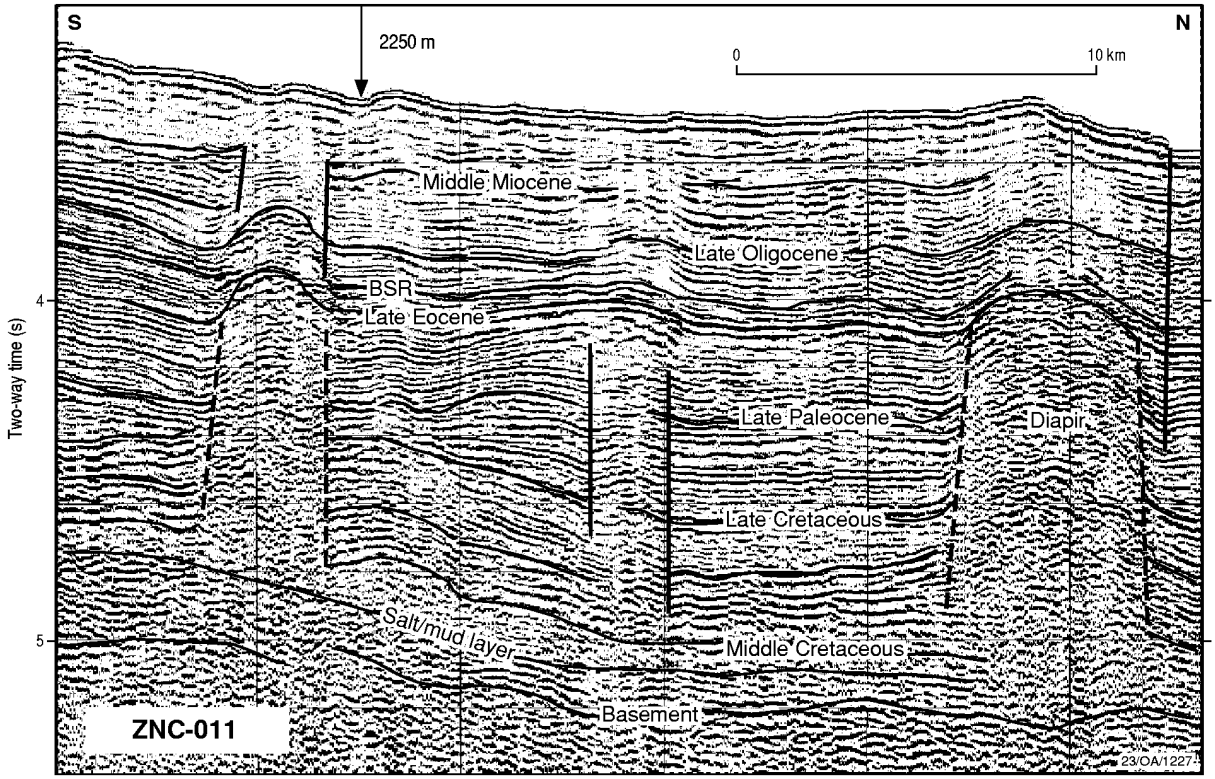

Figure 4. Seismic profile from the ZoNéCo 5 cruise (line 00/786-5) showing relationships between sediment diapirs, the BSR and faults on the seafloor in the SFB. Also labelled are the reflectors between inferred sediment packages (from Auzende *et al.*, 2000b).

The seafloor of the SFB has an unusually rough topography with probable pockmarks and fault scarps, some with more than 5 m of relief. Certain pockmarks are especially interesting because they overlie apparent faults and shallowings of the BSR. Where these relationships have been observed elsewhere, they signify upward movement of warm CH_4-charged water along faults, and subsequent gas venting on the seafloor (e.g., Westbrook *et al*., 1994; Paull *et al*., 1995; Taylor *et al*., 2000).

The region of diapirs and faulting in the SFB broadly coincides with the region of BSRs (Auzende *et al*., 2000b), suggesting a connection between the phenomena. With available data, the best explanation for the observed seismic features is a model that incorporates tectonics and gas (Auzende *et al*., 2000b):

(1) organic matter, mud, and perhaps salt, are deposited in a shallow rift basin during the mid-Cretaceous,
(2) the basin subsides and fills with several kilometres of sediment during the Late Cretaceous and early Paleogene,
(3) thermogenic gas, diapirs and faults are generated in the basin because of compaction and Eocene compression,
(4) gas hydrate forms at shallow depth through the upward flow of thermogenic gas along diapirs and faults, and
(5) some gas escapes to the seafloor along faults, creating pockmarks.

If this model is correct, the SFB is somewhat analogous to Mesozoic basins on other rifted margins with significant quantities of thermogenic gas, gas hydrate, diapir-related flow, and hydrocarbon seepage, notably basins in the Gulf of Mexico (e.g., Kennicutt & Brooks, 1990). The radarsat anomalies may represent liquid hydrocarbon slicks resulting from inferred seafloor venting, although no evidence of hydrocarbons was found in near-surface waters by fluorescence and absorption spectroscopy during the ZoNéCo 5 cruise (Holdway *et al*., 2000). Interestingly, however, a recent cable route swath-mapping survey revealed a huge flowing mud volcano on the eastern flank of the Lord Howe Rise, suggesting a massive escape of fluids from depth (Dr Loren Kroenke, pers. comm.).

The SFB may be a frontier hydrocarbon province of special interest to Australia and France. However, very little is known about this region, including the composition of sediment, gas and pore water. Thirteen piston cores were collected from the SFB during the ZoNéCo 5 cruise, primarily to investigate possible relationships between the shallow sediment system and the BSR. In this report, we describe this first set of piston cores from the SFB.

[*Note that coloured versions of the figures are included in the CD-ROM*]

3. SITE LOCATIONS

The ZoNéCo 5 cruise was primarily an extensive bathymetric and geophysical survey of the northeast LHR. In total, the survey covered approximately 100,000 km^2 within the New Caledonia Exclusive Economic Zone (EEZ) between 22° and 27° S and 162°30 and 165°30 E (**Fig. 1**). Much of the cruise was dedicated to mapping the BSR in the SFB, and searching for unusual tectonic or sedimentary features with a combination of multibeam echosounding, side-scan imaging, 6-channel seismic reflection profiling, and 3.5 kHz sub-bottom profiling. However, on two separate occasions, nearly a full day was devoted to piston coring in order to understand the nature of the BSR and seafloor sediments in the SFB.

Thirteen piston cores were taken from an area between 25°30 and 26°40 S and 163°25 and 164°30 E (**Figs. 5, 6, 7**). One set of seven cores (KG01 – KG07) was collected in the north-east section on October 27-28; a second set of five cores (KG09 – KG13) was collected in the

southwest section on October 31. These 12 locations were chosen to target specific features identified on ZoNéCo 5 geophysical records across the SFB (**Table 1**). One core (KG08) was also collected on October 30 to provide a sediment reference section on the flank of LHR outside of the SFB. GPS navigation, dynamic positioning and good weather ensured that all targets were sampled precisely. Sediment thickness at the 13 sites varies from less than 1 km at KG01 and KG08 to about 3 km at other sites (**Table 1**). For each site, a Kullenberg piston corer of 10 m length was used with a weight of 1300 kg and a core diameter of approximately 8.5 cm. The equipment was reliable and gave good penetration into very sticky sediment. Indeed, the only failure came at the location of core KG05 when the successful Russian-designed core head with two core catchers was replaced with a conventional core head with only one catcher. In this case, the core catcher turned inside out, the original core escaped, and a new core had to be collected. Pull-out force ranged from 1000 to 2000 kg. Cores were virtually undisturbed, although a broken saw damaged sections of KG13 during splitting.

Table 1. Locations and targets for *ZoNéCo 5* cores

Core	Date* (d/m)	Time§ (h:m:s)	Latitude (°S)	Long. (°E)	Depth‡ (mbsl)	Total sed. (m)*	Neogene sed. (m)*	Target Description
KG 01	19/10	14:11	25 35.74	164 28.58	2735	2000	400	Pock mark, BSR, fault
KG 02	19/10	13:42	25 30.27	164 27.55	2753	1000	400	Pock mark, BSR, fault
KG 03	20/10	03:05:30	25 37.64	164 19.20	2653	2500	400	Pock mark, BSR, fault
KG 04	20/10	02:33:30	25 43.26	164 20.35	2647	3000	400	Pock mark, BSR
KG 05	21/10	05:18	25 39.80	164 11.07	2604	3000	450	Hard Quaternary sequence, BSR
KG 06	21/10	05:58	25 46.33	164 12.23	2530	3000	500	Pock mark, BSR, fault, diapir
KG 07	21/10	06:30	25 51.70	164 13.30	2569	3000	450	Pock mark, BSR, fault, diapir
KG 08	29/10	08:15	26 19.80	163 23.70	1250	250	250	Background core on LHR basement
KG 09	-	SP 20517	26 38.60	164 14.00	2473	3000	500	Flat spot, fault, seepage
KG 10	23/10	01:51	26 32.64	164 05.35	2390	3000	550	Domed BSR, fault, diapir
KG 11	23/10	05:41	26 19.64	163 54.89	2060	3000	500	Pock mark, BSR, diapir
KG 12	23/10	06:01	26 16.50	163 54.24	2031	3000	450	Intense backscatter, BSR, fault
KG 13	23/10	07:42	26 00.77	163 51.31	1968	2000	450	Pock mark, deep fault, BSR

Notes: All cores were taken in 1999; *Date and §time are those recorded on ZoNéCo seismic profiles, rather than the date the core was taken, except for Core KG 09 which lies at shot point 20517 on *RV Rig Seismic* Line LHRNR-BA; ‡depth = water depth in m below sea level; †sed. = sediment thicknesses estimated from seismic profiles.

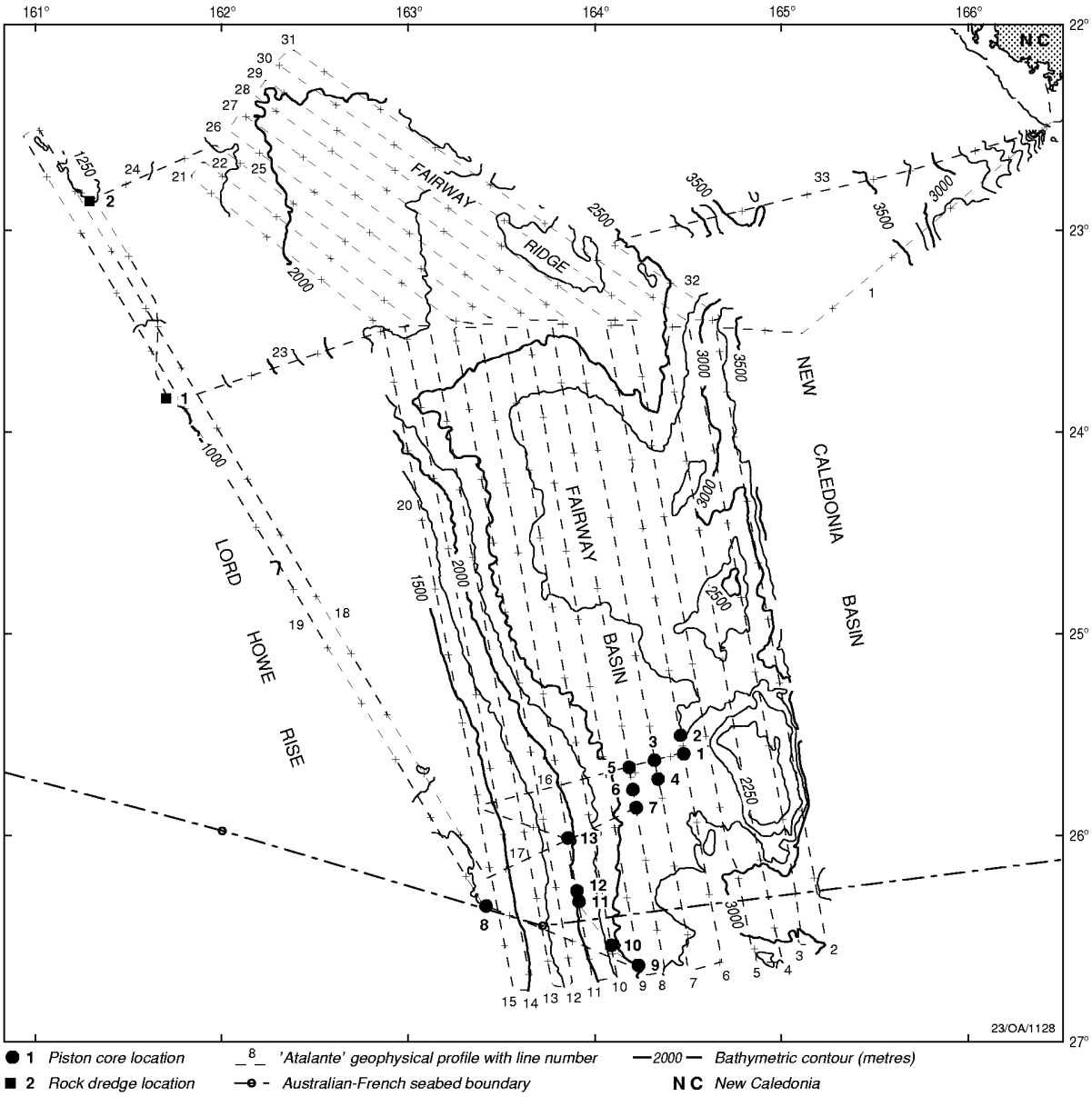

Figure 5. Bathymetric map of the ZoNéCo 5 survey area (**Fig. 1**) based on multibeam sonar sounding, showing seismic lines and locations of the 13 piston core sites.

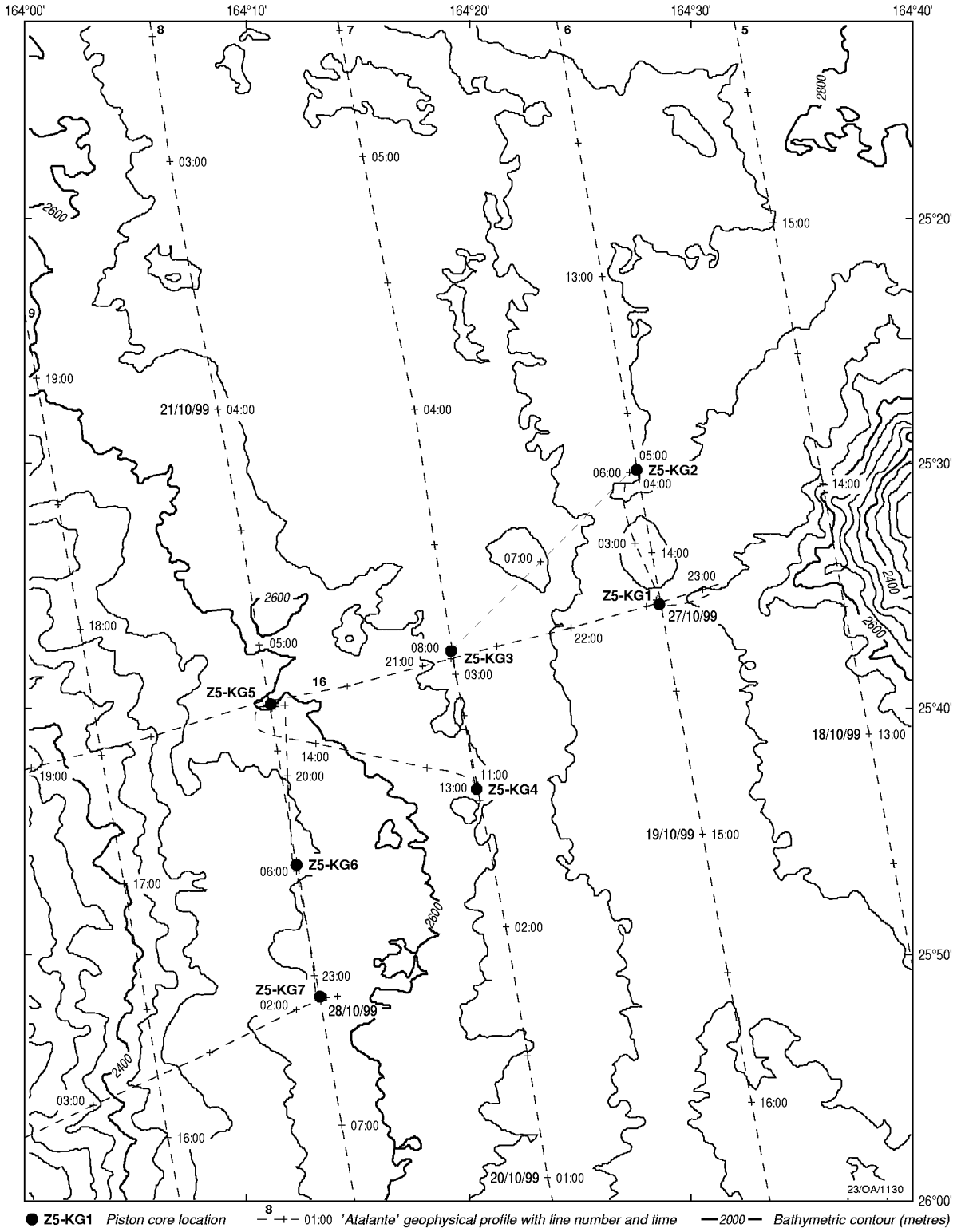

Figure 6. Detailed bathymetric map of the northeast area showing seismic lines and locations of cores KG01-07. Bathymetry based on multibeam sonar sounding.

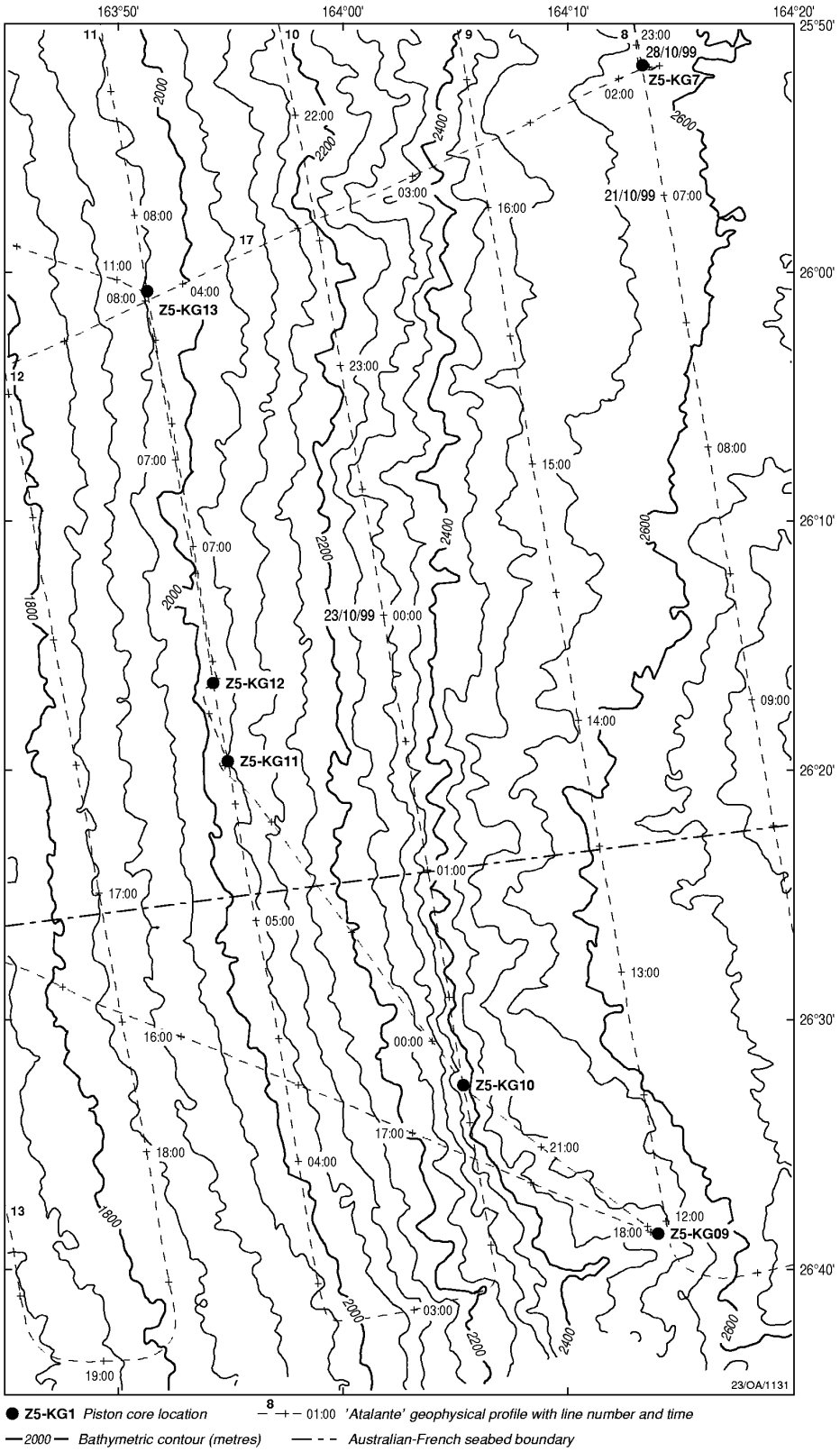

Figure 7. Detailed bathymetric map of the southwest area showing seismic lines and locations of cores KG07-13. Note that the site of core KG-08 lies west of this area (**Fig. 5**). Bathymetry based on multibeam sonar sounding.

4. SHIPBOARD SAMPLING AND ANALYSES

Core handling and description

Recovered cores were measured on the deck and cut into sections approximately 1 m long. Each section was split into a "working half" and an "archive half". The working half was sampled for sediment and pore water analyses, while the archive half was logged and described. Colours were determined on wet sediment using a Munsell Rock Colour Chart, and smear slides were made at representative intervals to guide sediment description.

Canned samples for gas analysis

One shallow and one deep sample generally were taken from each core to investigate the molecular and isotopic composition of gas according to a procedure developed by Keith Kvenvolden (USGS, pers. comm.). A piece of half-core with diameter of 9.5 cm and length 10 cm (about 300 cm^3) was placed in a 500 cm^3 paint can with a septa and covered with clean sea water until the can was full. Precisely 100 cc of water were removed with a syringe to get a known volume of headspace. One cm^3 of $HgCl_2$ was added to kill bacteria. Two needles were then placed into the septa and the headspace was purged with helium for several minutes at low pressure. The can was hammered shut, shaken to mix in the bactericide, and frozen upside down for transport back to AGSO. Sediment samples were canned within 30 minutes of splitting the core to reduce degassing at atmospheric pressure and room temperature, but the average delay in sampling after core recovery was an hour for shallow samples and two hours for deep samples.

Bottled samples for biomarker analysis

One shallow and one deep sample also were taken from most cores to analyse for potential hydrocarbon biomarkers. About 150 cc of sediment were added to a 500 cc plastic bottle. The samples were then sealed and frozen with no bactericide for subsequent analysis by solvent extraction and gas chromatography-mass spectrometry.

Pore waters

A total of 59 pore water samples were taken using a squeezing apparatus consisting of a nitrogen tank, a brass gas manifold, and a series of pressure chambers made of heavy plastic, each with a hole in the bottom covered with a wire mesh and filter. For each pore water sample, a furrow was cut into the centre of a split core with a clean knife. About 100 cm^3 of sediment was collected and packed into one of the pressure chambers. The chamber was sealed with a clamp. Nitrogen at pressure was passed through the manifold and into the sediment-filled chamber, squeezing pore water through the hole into a second filter and empty syringe. A nitrogen pressure of 1.9 bars typically produced about 7 to 10 ml of pore water, although for some samples, less than 5 ml. Pore waters were injected from the syringes into plastic vials, sealed, and stored in a refrigerator. Between three and seven pore water samples were taken from each core. For three pore waters, two sets of samples were taken. In addition, 4 aliquots of a seawater sample were collected, stored and shipped with the pore water samples. This seawater had an average S = 34.6, as determined by passing water through an environmental data logger which continuously measured conductivity and hence salinity.

Post-cruise shipping

The working and archive core halves were covered with saran wrap, reconnected and placed into a refrigerator on the *L'Atalante* along with the pore waters. The pore waters were shipped from the *L'Atalante* to Townsville cold at the end of the ZoNéCo 5 cruise; the sealed cores were shipped from the *L'Atalante* to Townsville cold in January, 2000.

5. SHOREBASED METHODS AND ANALYSES

Visual reflectance (greyscale)

Greyscale is a parameter for the visual reflectance or "greyness" of sediment. In pelagic sediment, greyscale often relates to carbonate content because the reflectance of carbonate minerals in the visible spectrum is much higher than for most non-carbonate phases (e.g., Mix *et al.*, 1995). Greyscale measurements can thus offer a rapid and non-destructive technique for correlating lithological variations (e.g., Cortijo *et al*., 1995; Adkins *et al.*, 1997; Dunbar *et al*., 2000).

Individual sections of core from the archive halves were scraped to remove surface water and to smooth exposed surfaces. A background white calibration strip and a Kodak greyscale reference chart (Kodak publication number Q-14) were placed next to each core section. A digital image was then acquired using a Kodak DC-40 camera. Lighting provided by four GEC-Osram 150 W Quartz-Iodine bulbs containing tungsten filaments. Colour was corrected to "daylight" using an 80A filter.

Sediment greyscale was determined from the digital core images. Images were downloaded to a PC, and greyscale values were obtained using the public domain software package "NIH Image v 1.60". Greyscale measurements were averaged across a width of 30 pixels (4.5 mm) from the centre of the core. The positions of core sections, camera, and lights were kept constant for all images, and variations in illumination along the length of the core were eliminated as much as possible by normalising image greyscale intensity to variations in the intensity measured along the uniform white calibration strip. Greyscale values were then scaled accordingly from 0.0 (100 % black) to 1.0 (100 % white). Previous work using this method has shown that absolute greyscale values change over time as cores dry and oxidise, but that relative greyscale values on single cores are robust for at least one year (Dunbar *et al*., 2000).

Volume magnetic susceptibility

Magnetic susceptibility (MS) is a measure of the magnetic response of a material to an external low-strength magnetic field (Thompson & Oldfield, 1986; Hunt *et al*., 1995). This parameter is typically expressed as a ratio of the magnetisation induced in the sample per unit volume to the strength of the applied field (e.g., Hunt *et al*., 1995). Sediment MS is commonly used to correlate lithological variations in pelagic sediment cores (e.g., Robinson, 1993; Dickens *et al*., 1995; Dunbar *et al*., 2000).

Magnetic susceptibility was measured on the archive halves of all 13 cores using a GEOTEK multi-sensor track system. The split cores were equilibrated at room temperature (nominally 25°C), and sediment MS was measured at a spacing of 4 mm using a Bartington Instruments MS2 meter connected to a Bartington "F" type point sensor unit with a spatial resolution of approximately 20 mm. The MS2 meter measures susceptibility using a tuned oscillator circuit. Variations in the frequency of the AC waveform caused by placing the sensor on magnetically susceptible sediment are directly proportional to the MS of the sample (Robinson, 1993). Our system was operated with an AC field strength of 80 A/m rms, and at a frequency of 0.58 kHz (1 s integration time). The MS meter is controlled by a microprocessor

that raises the sensor 20 mm above the core surface and re-zeros the meter between readings to minimise drift. Volume MS data for all cores are reported in arbitrary Bartington Meter SI scale units. Previous work on marine sediment cores using this method indicates that MS measurements are reproducible to within 1.5 SI (Dunbar *et al.*, 2000)

Pore water sulphate and chloride

The 59 pore water and 4 seawater samples were analysed for SO_4^{2-} concentrations by the turbidimetric method where $BaSO_4$ precipitation affects the penetration of light through water. Approximately 0.05 ml of sample was mixed with deionised water to 50 ml total volume. These solutions were placed into a spectrophotometer and measured for light penetration at 420 nm wavelength. Approximately 150 mg of $BaCl_2$ and 10 ml of a buffer solution were added. The solution was stirred for 1 minute and then let stand for 5 minutes. The solutions were again placed into a spectrophotometer and measured for light penetration at 420 nm wavelength. Sulphate concentrations were determined by calibrating light penetration to that of known standards. Concentrations of the three "replicate" samples were within 0.8 mM and the seawater samples had a SO_4^{2-} concentration of 27.2 ± 0.5 mM.

Ten pore water samples were analysed for Cl^- concentrations by the argentometric method. Approximately 0.05 ml of sample was mixed with deionised water to 50 ml total. One ml of $KCrO_4$ solution was then added to an aliquot of each sample. While stirring, drops of $AgNO_3$ titrant were added until the colour became pinkish-yellow. Chloride concentrations were determined by from the amount of titrant used. One sample was analysed twice to evaluate precision; these replicates both had a Cl^- concentration of 533 mM.

Gas composition

Analyses of headspace gas samples were carried out using a Hewlett Packard 5890GC equipped with a gas sampling loop (1ml). Headspace gas (5ml) was sampled through the septum on the tin cans and manually injected onto the sample loop. The sample was split at the injector and passed through two columns. Column one was a 30m x 0.53 mm ID AT-Q (Alltech Cat# 13939) connected to a flame ionisation detector (FID) to analyse C_1-C_7+ hydrocarbons. Column two was a 1.8m CRT 1 column (Alltech Cat# 8700) connected to a thermal conductivity detector (TCD) to analyse the inert gases and methane. The GC conditions used for these analyses are listed in **Table 2**. Gas concentrations were quantified through comparison to an external natural gas standard supplied by BOC gases.

Table 2. Conditions for Gas Chromatography Analyses

Sampling valve temp	150°C
Injector temp	200°C
Detector temperature (TCD)	160°C
Detector temperature (FID)	200°C
Initial oven temperature	60°C (1minute)
Oven ramp rate	15°C /min
Final oven temperature	160°C
Column head pressure (helium)	40psi

Attempts were made to analyse the carbon isotopic composition of CH_4 in samples from the lower parts of cores KG 02 and KG 03. However, there was insufficient gas.

Higher (C7+) hydrocarbons

Solvent extraction was conducted on five samples from cores that had high concentrations of wet gas components (KG 02 142-150, KG 02 461-469, KG 03 121-129, KG 03 511-519 and KG 10 548-552). On completion of gas analyses, the lids were removed from each container and approximately half the contents were transferred to a 500ml separating funnel for extraction with dichloromethane (2x 90ml). This process was repeated with the remaining half. The combined extracts (350ml) were reduced *in vacuo* to 1ml, an internal standard added (5µg iso-C_{22} alkane) and the sample analysed by Gas Chromatography-Mass Spectrometry using an HP 5973 instrument fitted with a DB-5 column (50m x 0.22mm ID). The injector GC was operated in the splitless mode using He as carrier, and the oven was programmed from 60-320ºC at 6ºC/min.

6. SHIPBOARD RESULTS AND DISCUSSION

The 13 sediment cores varied in length from 405 to 758 cm and averaged 635 cm (**Table 3**). All cores contain very stiff sediment with a similar colour sequence (**Plates 1-13**). The normal Munsell colour sequence is greyish orange (10YR7/4) at the top, very pale orange (10YR 8/2) in the middle, and then either yellowish grey (5Y 8/1), very light grey (N8) or white (N9) at the bottom with occasional intervals of very pale orange (10YR 8/2. Most colour changes are gradational. Bioturbation is subtle, occurring in the form of light mottles and 1-2 cm wide horizontal and vertical burrows in shallow sediment, and as pyritic burrows and flecks at depth. Occasional pumice granules are present. Gas voids were not observed in any of the cores.

Table 3. Sediment units in the *ZoNéCo 5* cores

Core	Length (cm)	Greyish orange/ very pale orange transition (cm)*	Top depths of discrete green/yellow horizons transition (cm)*	Top Orange/ grey transition (cm)	PI/PII Boundary (cm)	PII/PIII Boundary (cm)
KG 01	682	197	Not observed	Not observed	197	635
KG 02	602	210	495	Not observed	162	Not observed
KG 03	688	205	445	Not observed	140	638
KG 04	610	240	437	Not observed	194	565
KG 05	735	227	429	437	136	437
KG 06	702	158	423, 429?, 443	466	158	466
KG 07	430	160	314	318	145	340
KG 08	683	Gradual	638	Not observed	Not observed	Not observed
KG 09	425	142	362, 375	389	142	389
KG 10	648	140	339, 367	432	140	Not observed
KG 11	583	140	432, 470	500	140	519
KG 12	758	146	417, 439, 443	643	146	643
KG 13	703	130	505	535	130	535

Notes: *Shipboard colour determined using the Munsell chart. PI, PII, PIII = sediment intervals defined by physical property measurements (see text)

Two marker horizons are present in most cores (**Table 3, Plates 1-13**). First, the greyish orange to very pale orange transition occurs over a fairly well defined interval in all cores between 130 and 240 cm except core KG08. This transition is apparent in core KG08 but too gradual to assign a depth with a Munsell chart. Second, from one to three yellowish-green (general not Munsell term) horizons (<2 cm), much like those described from DSDP Leg 90 in the region (Gardner et al., 1986), are present in all cores except KG01. Given stratigraphic

relationships (discussed below), the horizon may occur between sections 5 and 6 at 430 cm in core KG01. A lower orange/grey transition also occurs in most cores between 310 and 650 cm. However, it is difficult to assign a depth to this horizon with a Munsell chart.

The yellowish-green horizons always lie between the upper and lower colour transitions. Relative to the upper colour transition, the top yellowish-green horizon is lower by 154 to 375 cm (excluding cores KG01 and KG08 that lack appropriate data). Interestingly, the upper yellowish-green horizon is shallowest in cores from intermediate water depths (~2400 to 2600 mbsl) and deeper in cores from shallower and deeper sites (**Fig. 8**). Moreover, only cores from between 2000 and 2600 mbsl have more than one yellowish-green horizon (**Tables 1 and 3**).

Sediment in the cores predominantly consists of nannofossils with subordinate and variable amounts of foraminiferal tests and clay. Pelagic foraminiferal tests are well preserved and decrease in abundance down the core so that the uppermost sediment is foram nannofossil ooze (>15% foraminiferal tests) and lower sediment is foram-bearing nannofossil ooze (5-15% foraminiferal tests). The nature of the planktonic foraminiferal assemblage also appears to change with depth between warm water (thin walled) and cool water (thick walled) types. Organic linings are still present in the foraminiferal tests in the upper part of the cores. Trace amounts of pyrite (including fillings of foraminiferal tests in some horizons), muscovite, palynomorphs, plate-like diatoms, sponge spicules and ascidian spicules are present in some samples. The sponge spicules are both calcareous and siliceous. In terms of grain size, the sediment is bimodal, with nannofossils and clay minerals forming a dominant clay fraction and foraminiferal tests forming a sand fraction.

Cores recovered by the ZoNéCo 5 cruise are not unlike the few other cores from the surrounding region. White, light grey, pale yellowish grey and light brownish grey calcareous oozes were cored by the R.V. *Sonne* at 1300 to 1400 mbsl on the LHR approximately 550 km to the southwest (Hinz *et al*., 1985). At DSDP Site 208, at 1545 mbsl on the LHR approximately 200 km to the west, sediments are greyish orange (10YR7/3) and very pale orange (10YR 8/2) in the top 10 m and gray white (5Y 9/1) below (Burns *et al*., 1973). At DSDP Site 588, at 1533 mbsl and near Site 208, sediments are greyish orange (10YR7/4) and very pale orange (10YR 8/2) in the top 6.8 m and white (N8) below (Shipboard Scientific Party, 1986). Possible green ash horizons were also noted in the upper 10 m (Shipboard Scientific Party, 1986). Sediments at both Sites 208 and 588 are described as calcareous spicule-bearing, foram-rich nannofossil ooze.

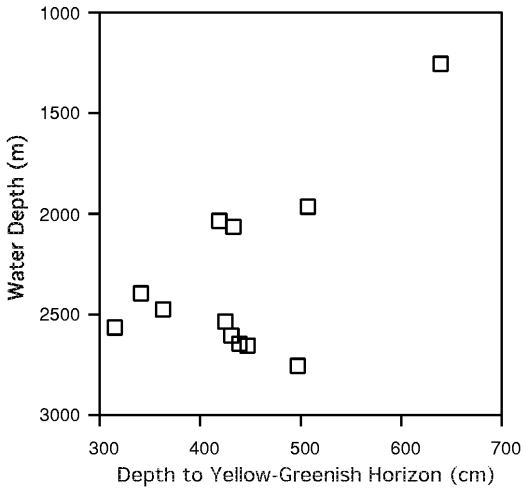

Figure 8. The depth below the sea bed of the highest yellowish-green horizon in the cores.

The three marker horizons may represent primary sedimentary features. In particular, the upper greyish orange to very pale orange transition may correspond with the boundary between foram nannofossil ooze and foram bearing nannofossil ooze, and the yellowish-green horizons may represent altered volcanic ash layers like the 'pale green laminae' described by Gardner et al. (1986). Highly weathered greenish-grey "pebbles" were found at 439 cm in core KG11 and 735 cm in core KG12. Although these pebbles are composed mostly of clay, they were probably originally basic glasses because they contain some euhedral crystals of pyroxene, hornblende and plagioclase. Pumice grains were also found at 262 m in core KG09 and 206 and 338 m in core KG12. However, it is not clear whether the green pebbles, pumice grains and yellowish-green sediment horizons are of the same composition.

Decreasing oxidation states could also lead to marker horizons in the sediment. In particular, the general loss of orange colour down the cores might represent the conversion of +3 Fe to +2 Fe after O_2 and NO_3^- have been removed from pore water (e.g., Froelich *et al*., 1979). Likewise, the green horizons could represent discrete redox fronts where a mineral phase is precipitating (e.g., Thomson *et al*., 1993; Dickens, 2001). Different oxidation states in the sediment could relate to water depth if fluxes of reduced carbon are highest in the central SFB. Upward transport of CH_4 from depth is a process that increases the supply of reduced carbon to shallow sediment (e.g., Borowski *et al*., 1999; Fossing *et al*., 2000).

One means to discriminate between possible origins for the marker horizons are sedimentation rates. If the marker horizons represent primary sedimentary features, locations at intermediate water depths in the SFB with closely spaced horizons should have significantly lower sedimentation rates than sites at shallower or deeper water depths. The opposite would be expected if the marker horizons were redox boundaries. The 250 m inferred Neogene sediment package beneath core KG08 on the LHR suggests an average sedimentation rate of approximately 10m/my. This is the same rate that was determined at DSDP Site 588 on the LHR by detailed biostratigraphy over 450 m of core (Shipboard Scientific Party, 1986), suggesting that seismic profiles can be used to estimate sedimentation rates in the region. Neogene sediment thicknesses in the SFB are highest beneath locations at intermediate water depth **(Table 1)**, arguing against a primary origin for the marker horizons.

The Tasman Front manifests itself as an eastward zonal jet between 152° and 173 ° E longitude, connecting the East Australian Current with the East Cape current northeast of New Zealand (Warren, 1970). Surface waters of this frontal zone are characterised by an abrupt change in temperature and foraminiferal assemblages (Heath, 1985; Martinez, 1994). At present, the TF lies significantly south of the SFB between 31 and 32.5 °S latitude for most of the year (Mulhearn, 1987). However, Martinez (1994) has argued on the basis of foraminiferal assemblages that the Tasman Front migrated to about 26 °S during the last glacial maximum or above the SFB. The general downcore change in foraminiferal assemblages from thin-walled to thick-walled tests may support this paleoceanographic scenario.

7. SHOREBASED RESULTS AND DISCUSSION

Physical Properties

The greyscale of cores from the SFB ranges from 0.5 to 0.95 (**Plates 1-13**). In general, the upper greyish orange interval has a greyness <0.8, the middle very pale orange interval has a greyness between 0.85 to 0.95, and the lower interval has a greyness <0.85 (**Fig. 9**). Many of the pyrite horizons show a significant drop in greyscale reflecting their dark nature.

Magnetic susceptibility ranges from 0 to >25 SI but is typically between 3 and 15 SI (**Plates 1-13**). Again, there is a general correspondence between MS and colour (**Fig. 9**). Usually the upper greyish orange interval has an MS between 5 and 15 SI, the middle very pale orange has a an MS <5 SI, and the lower interval has an MS between 5 and 10 SI. Overall, the MS decreases down cores.

The most striking feature about the MS records is a series of major increases, or spikes, in the middle colour interval between 200 and 400 cm (**Fig. 10**). These spikes are most prevalent in cores from the northeast section, less pronounced in cores from the south central section, and absent in core KG08 on the LHR (**Fig. 10**). As with the coloured horizons discussed above, the MS spikes could be primary signals reflecting changes in lithology or diagenetic intervals representing mineral precipitation, specifically magnetite. The formation of single-domain magnetite by bacteria is a well-documented process to generate prominent MS spikes in shallow sediment (e.g., Karlin & Levi, 1983; Bloemendal *et al*., 1988; Dickens & Owen, 1996).

Both the greyscale and MS records are considerably more detailed than the shipboard colour logs. Because all three records are somewhat correlated, it is possible to quantify boundaries between sediment units using the physical property records instead of the Munsell chart. The upper greyish orange to very pale orange transition occurs where the MS decreases by 5 to 10 SI after the greyness increases by 0.05 to 0.1 to greater than 0.70. By contrast, the lower orange/grey transition occurs where the greyness begins to decrease and MS increases by 5 to 10 SI. The colour boundaries are redefined in **Table 3** and **Plates 1-13** using these properties. Even with this approach, colour boundaries cannot be readily assigned for core KG08. This may highlight problems in using physical property measurements for characterising cores in the SFB, at least with available data. In particular, pale orange is not readily discernible from certain shades of grey. This means that orange has to be distinguished using MS under the assumption that some physical property of orange sediment gives rise to a higher MS than for grey sediment. However, MS could be low in grey sediment because of carbonate dilution or iron remobilisation.

Pore waters

Pore water SO_4^{2-} concentrations vary from 22.6 to 29 mM (**Table 4**). The higher concentrations of 27.5 to 29 mM are within the range of typical seawater. Considering all samples together, SO_4^{2-} concentrations are poorly correlated to sediment depth, although deeper samples have lower SO_4^{2-} concentrations overall (**Fig. 11**). The high degree of scatter is not caused by evaporation in certain samples, because all samples analysed have fairly similar Cl^- concentrations between 533 and 561 mM.

Individual cores appear to have a common trend in SO_4^{2-} concentrations with respect to depth. In general, SO_4^{2-} is high near the surface, low at shallow depth, high again at a deeper depth, and low toward the base (**Fig. 12**). A similar trend was reported at DSDP site 588 (Baker, 1986), although the sample resolution is low. There appears to be a correlation between sediment colour, MS and SO_4^{2-} concentrations (**Fig. 12**). Pale intervals with high greyness and low MS are characterised by low SO_4^{2-}. This may reflect aspects of organic matter decomposition. The oxidation of organic carbon in marine sediments commonly proceeds through a sequence of reactions including Fe oxyhydroxide reduction followed by SO_4^{2-} reduction (e.g., Froelich *et al*., 1979). Coloured oxyhydroxide phases with moderately low MS and some pore water SO_4^{2-} probably have been removed from "grey intervals", although some of the Fe has re-precipitated as magnetite or pyrite.

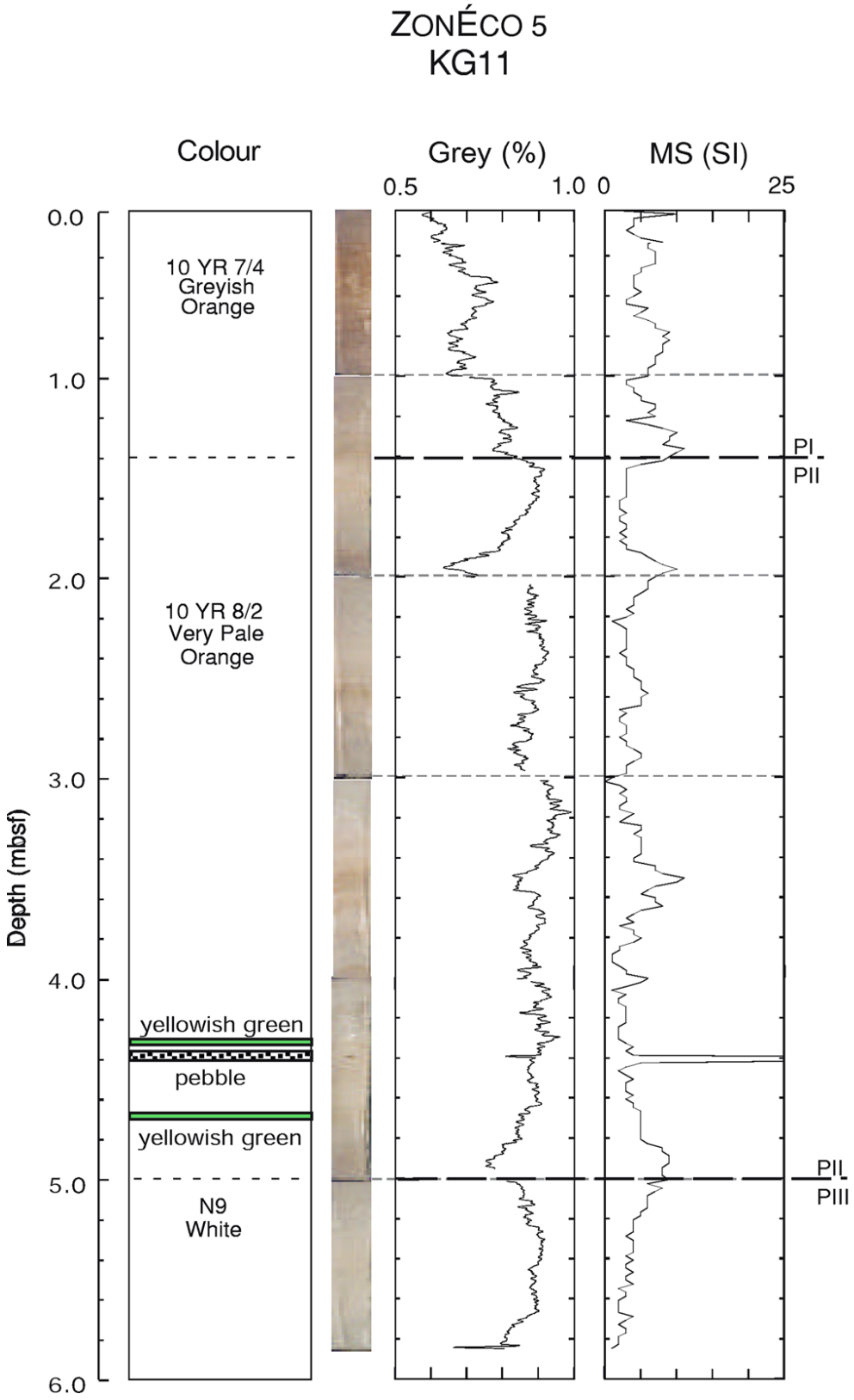

Figure 9. Relationship between colour, greyscale and magnetic susceptibility for core KG11.

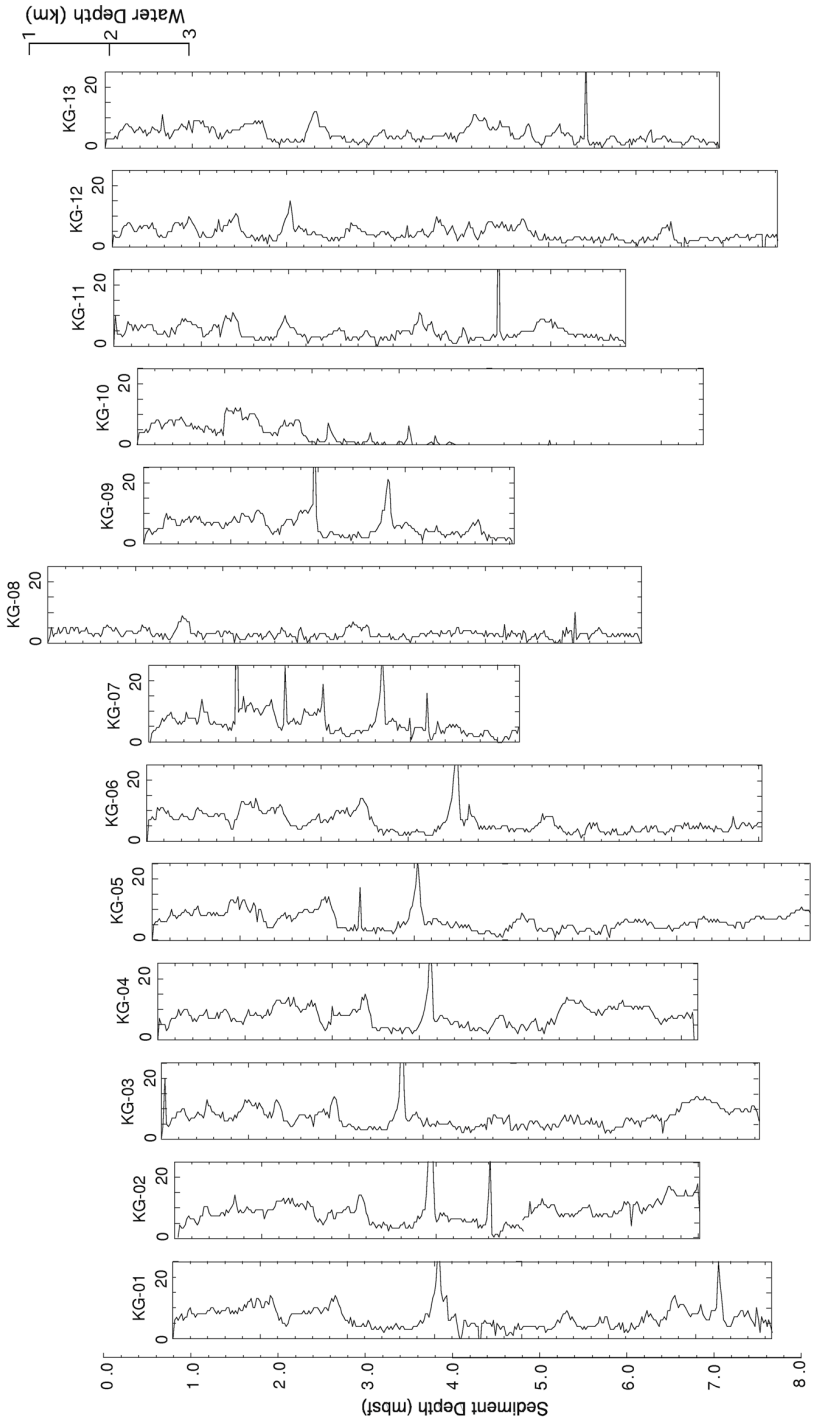

Figure 10. Magnetic susceptibility records for cores across the SFB staggered according to the water depth. Note the similarity of the records of northeastern cores KG01-06, and the similarity of the records of southwestern cores KG10-13.

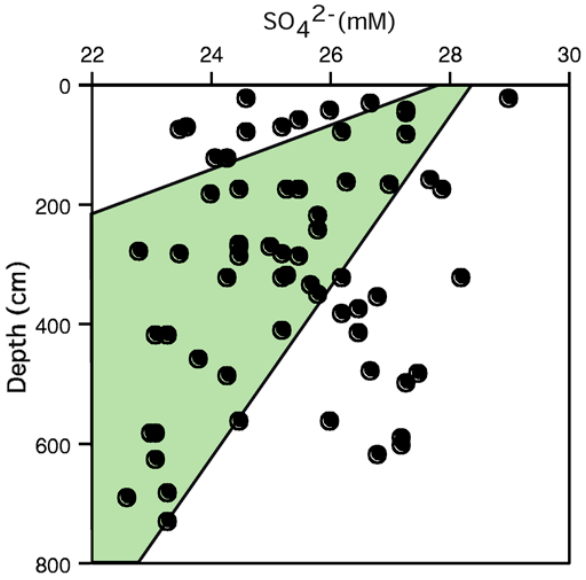

Figure 11. Sulphate concentrations of pore waters against sediment depth in the cores.

Upward flow of gas-rich fluids through the well-studied Blake Ridge gas hydrate deposit causes BSRs (Xu and Ruppel, 1998) and induces anaerobic CH_4 oxidation in shallow sediment, a process that consumes SO_4^{2-}. As a consequence, above BSRs, pore water SO_4^{2-} concentrations decrease linearly from seawater values at the seafloor to zero 10 to 20 m depth (Borowski *et al*., 1999; Dickens, 2001). Moreover, above marine gas hydrate deposits, there appears to be a strong spatial coincidence between the presence of BSRs and the steepness of SO_4^{2-} gradients and redox fronts (Borowski *et al*., 1999). The overall decrease in pore water SO_4^{2-} lies within the range observed on the Blake Ridge (**Fig. 11**). However, the profiles are not linear.

Gases

The results of the gas analyses are tabulated (**Table 5**) and presented graphically in **Figure 13**. The highest CH_4 concentrations were between 1.1 and 2.7 ppm in cores KG 02, 03, 07, 09, 10 and 13. In general, there is a trend toward higher gas contents with depth. Moreover, samples with the highest CH_4 concentrations also contained small amounts of ethane and propane (**Fig. 13**). These data suggest a thermogenic rather than biogenic origin for gases in the SFB. However, we were unable to support this idea through carbon isotope analyses because the abundance of all gaseous components was too low. Samples examined for higher hydrocarbons contained minute traces of n-alkanes in the C_{20+} range (<< 1 ppb). These n-alkanes showed no odd-over-even carbon number predominance (**Fig. 14**), which rules out plant wax as a source for these compounds. These results are certainly suggestive of the presence of thermogenic hydrocarbons but should be viewed cautiously until replicated. At these trace levels, contamination from fuels and lubricants is always a possibility.

Table 4. Pore water sulphate concentrations for sediment from the *ZoNéCo 5* cores

Core	Section	Top Depth (cm)	Bottom Depth (cm)	SO_4^{2-} (mM)	Core	Section	Top Depth (cm)	Bottom Depth (cm)	SO_4^{2-} (mM)
KG 01	B	43	50	27.3	KG 07	A	62	76	23.6
	C	211	221	25.8		B	176	153	27.0
	E	342	355	25.8		D	320	323	26.2
	G1	595	605	27.2		E	411	419	23.1
	G2	595	605	27.2					
					KG 08	C	262	273	24.5
KG 02	A	52	62	25.5		C2	262	273	25
	B	166	177	25.5		D	315	326	25.2
	D	366	376	26.5		F	611	635	23.1
	E	480	490	24.3					
	F	575	585	23.0	KG 09	A	23	31	26.7
						B1	114	130	24.3
KG 03	A	38	47	27.3		B2	114	130	24.1
	B	155	165	26.3		D	312	327	24.3
	C	234	246	25.8		E	405	415	25.2
	D	328	338	25.7					
	E	405	417	26.5	KG 10	A	14	27	24.6
	F	493	504	27.3		B	176	188	24
	G	584	594	27.2		E	474	484	27.5
						F	574	587	23.1
KG 04	A	74	89	27.3					
	B	168	181	27.9	KG 11	A	61	81	23.5
	C	257	271	24.5		C	276	290	25.5
	F	553	571	26.0		D	372	386	26.2
						F	553	566	24.5
KG 05	A	15	29	29.0					
	B1	168	180	25.3	KG 12	A	60	77	25.2
	B2	168	180	24.5		C	277	282	25.2
	C	277	290	24.5		E	471	482	26.7
	D	317	328	28.2		H	723	735	23.3
	E	410	423	23.3					
	G	610	620	26.8	KG 13	A	64	86	26.2
						C	272	289	23.5
KG 06	A	30	48	26.0		D	343	359	26.8
	B	157	159	27.7		F	675	685	23.3
	C	273	283	22.8					
	D	310	325	25.3					
	E	446	465	23.8					
	G	682	694	22.6					

Table 5. Composition of headspace gas in the *ZoNéCo 5* cores

Core	Top Depth (cm)	Bottom Depth (cm)	CH_4 (ppm)	C_2H_4 (ppm)	C_2H_6 (ppm)	C_3H_8 (ppm)
KG 01	142	152	0.20	0.00	0.04	0.00
KG 01	642	650	0.35	0.00	0.07	0.00
KG 02	142	150	1.52	0.00	0.41	0.38
KG 02	480	490	2.19	0.00	0.80	0.00
KG 03	139	149	0.77	0.00	0.32	0.00
KG 03	141	149	0.39	0.00	0.04	0.00
KG 03	511	519	2.08	0.23	0.12	0.08
KG 04	60	70	0.49	0.00	0.11	0.00
KG 05	600	610	0.44	0.00	0.13	0.00
KG 05	729	739	0.47	0.00	0.13	0.21
KG 06	180	190	0.03	0.00	0.00	0.00
KG 06	660	670	0.30	0.01	0.04	0.00
KG 07	80	90	1.57	0.00	0.07	0.00
KG 07	401	410	0.22	0.00	0.00	0.00
KG 08	59	60	0.30	0.00	0.00	0.00
KG 08	580	590	0.81	0.00	0.10	0.00
KG 09	80	90	0.63	0.00	0.21	0.22
KG 09	393	397	1.11	0.00	0.07	0.00
KG 09	415	422	0.27	0.00	0.04	0.00
KG 10	80	90	0.21	0.00	0.04	0.00
KG 10	559	560	1.67	0.00	0.49	0.41
KG 11	83	93	0.29	0.00	0.00	0.00
KG 11	569	579	0.59	0.00	0.06	0.00
KG 11	742	752	0.15	0.00	0.00	0.00
KG 12	82	92	0.49	0.00	0.00	0.00
KG 13	112	122	0.00	0.00	0.00	0.00
KG 13	675	685	1.09	0.09	0.06	0.00

8. CONCLUSIONS AND FUTURE RESEARCH

The SFB was a largely unexplored basin on the eastern flank of the northern LHR in the Tasman Sea. Recent geophysical cruises have discovered several intriguing features in this basin, including an extensive BSR suggestive of substantial amounts of gas hydrate and free gas below the seafloor. The French RV *L'Atalante* collected 13 piston cores of 405 to 758 cm length from this region in order to document the nature of sediment, pore water and gas in the shallow sedimentary section. The sediment is stiff nannofossil ooze with foraminiferal tests, typically grading from greyish orange (10YR7/4) at the top, to very pale orange (10YR 8/2) in the middle, and then to either yellowish grey (5Y 8/1), very light grey (N8) or white (N9) at the bottom. Some pyrite occurs in black horizons. At the same depth, cores from the south central part of the SFB are greyer.

The change in colour with depth is related to variations in MS. Specifically, pale and grey zones in cores from the SFB are characterised by generally low MS punctuated by a series of MS highs. Pore water SO_4^{2-} concentrations are also low in these sediment intervals. The best overall explanation for colour, MS and SO_4^{2-} profiles in sediment from the SFB is that Fe and SO_4^{2-} have been remobilised under anoxic conditions. After carbon remineralisation has consumed O_2 and NO_3^- from pore water, the small amount of +3 Fe in solid oxyhydroxide phases is converted dissolved +2 Fe and SO_4^{2-} is removed from pore water. Some of this Fe is re-precipitated as pyrite or magnetite (the MS spikes).

Upward fluxes of CH_4 through gas hydrate deposits induce anaerobic CH_4 oxidation in shallow sediment, a process that consumes SO_4^{2-}. As a consequence, redox fronts are shallower than expected from considerations of organic matter input to the seafloor. The relatively shallow redox fronts in the SFB may support enhanced CH_4 fluxes but additional data is needed.

The detection of wet gas components in some samples suggests that CH_4 in the SFB is associated with thermogenic processes. Minute traces of higher (C_{20+}) hydrocarbons were present but the low amounts precluded further classification. The three cores with appreciable quantities of higher hydrocarbons all occurred in association with deep faults and displaced sea bed, and domed BSRs (**Table 6**). Again, additional work on new cores is needed.

Dickens et al., Figure 12

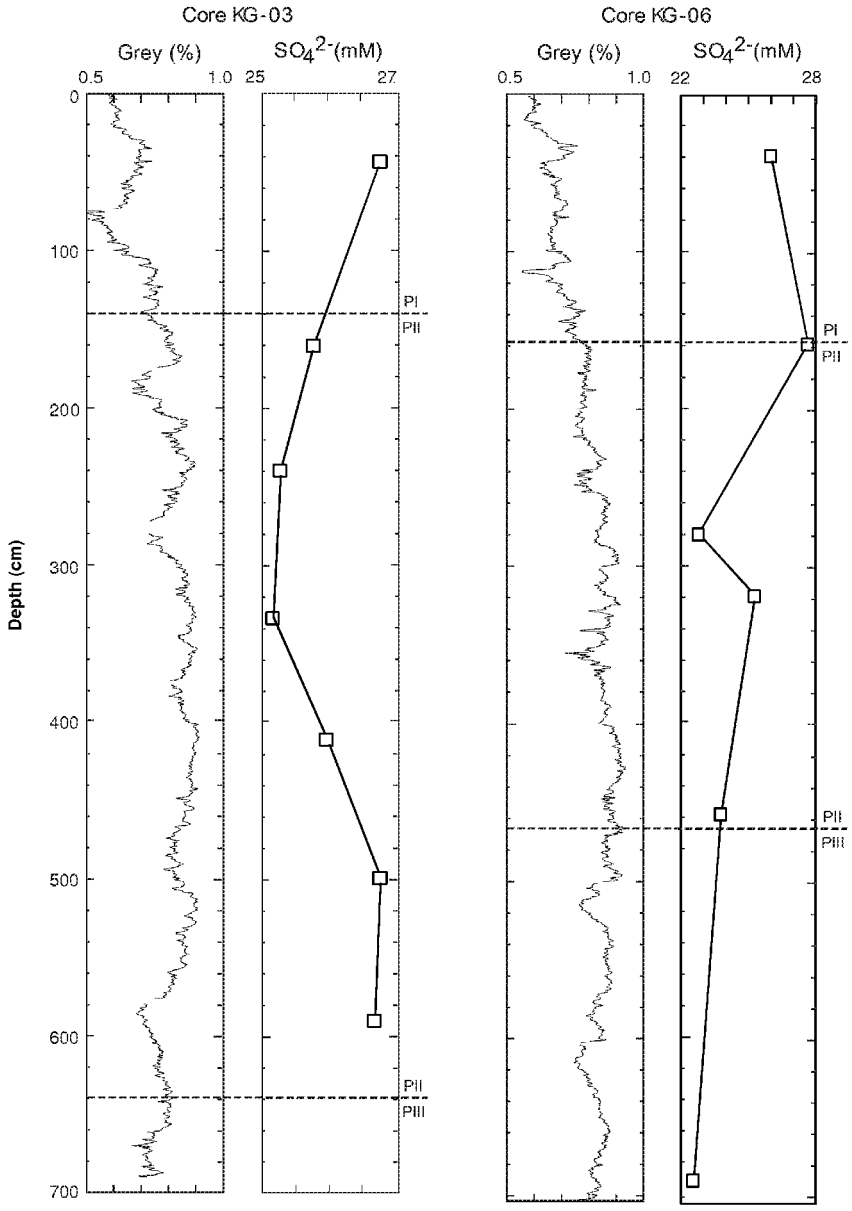

Figure 12. Relationship between greyscale and SO_4^{2-} concentrations with sediment depth in the pale unit II of core KG-03.

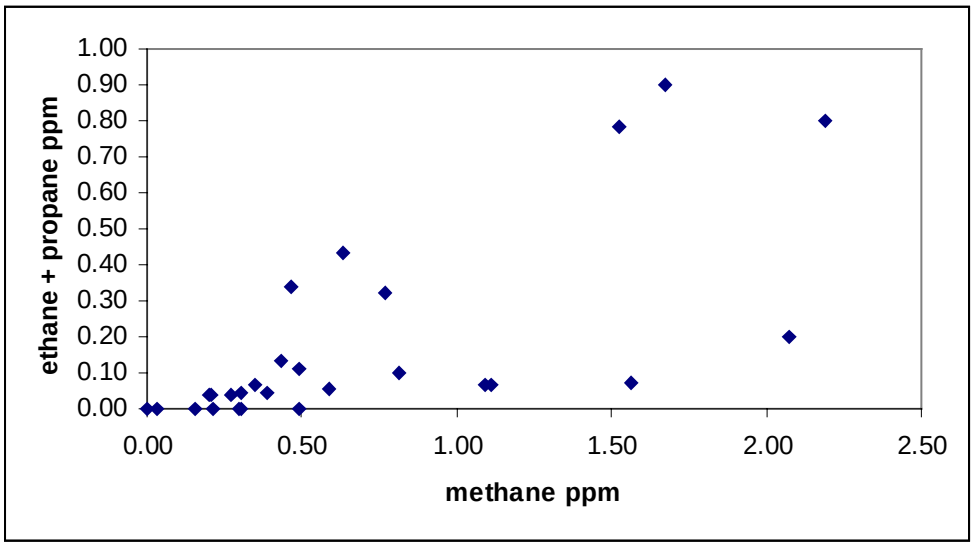

Figure 13. Gas composition cross-plot. The positive correlation between methane content and ethane plus propane content suggests a predominantly thermogenic origin for the gas.

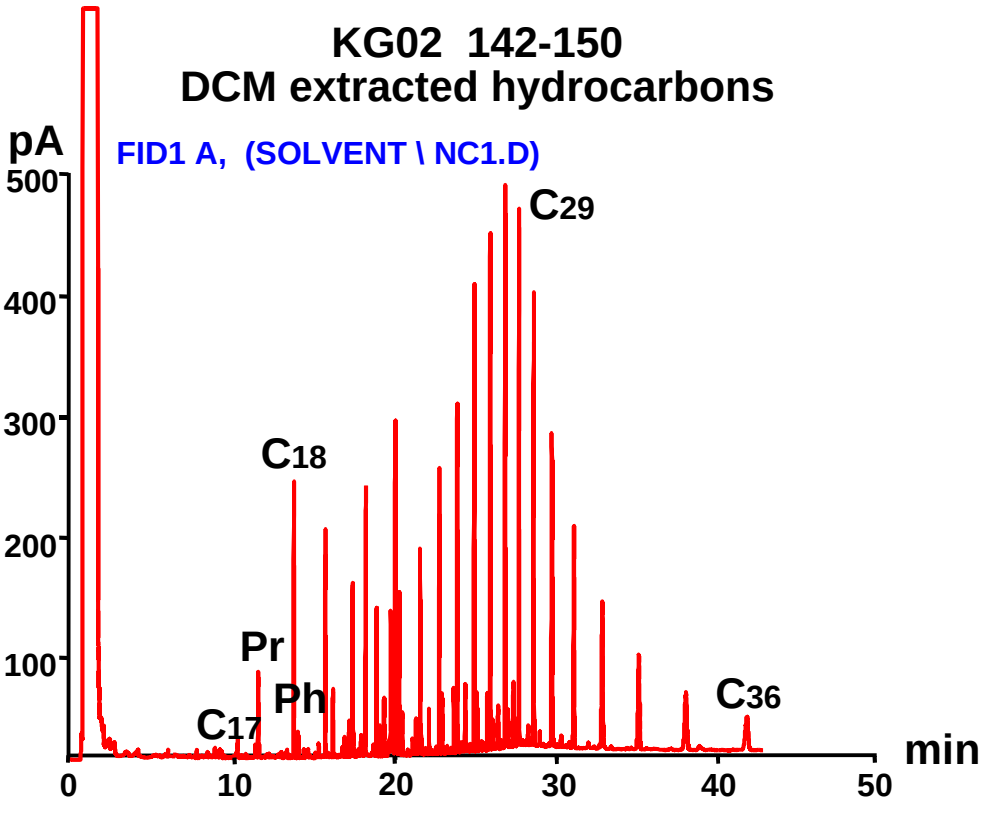

Figure 14. Gas chromatogram from core KG-02, suggesting that it contains waxy biodegraded hydrocarbons.

Table 6. Information on cores with relatively high wet gas content

Core	Water Depth‡ (m)	Total sediment (m)*	Location	Description
KG 02	2753	1000	Near eastern high	Moderately domed BSR, pock mark 10 m deep, possible fault
KG 03	2653	2500	Central basin	Slightly domed BSR, faulted depression 5 m deep
KG 10	2390	3000	Central basin	Base of strongly domed BSR and diapir, faulted depression 10 m deep, highly faulted surface with fault throws of up to 40 m

In late 2001, the CSIRO-operated RV *Franklin* will be used to significantly advance our knowledge of SFB, including the unexplored Australian sector (**Fig. 1**). Principal research objectives planned for this cruise include (Exon, Hill, Dickens & Lafoy, 2001):

(1) map sediment diapirs and BSRs in the Australian sector,
(2) tie basin sequences to existing DSDP holes via new seismic lines,
(3) determine the nature of sediment, pore waters and gas over a much larger region,
(4) dredge outcropping sequences to ground-truth seismic data,
(5) establish the Holocene and Pleistocene climate history above the SFB.

It is hoped that longer cores might be taken from this region in the future, perhaps from the *Marion Dufresne* and/or the successor to the Ocean Drilling Program (ODP) *JOIDES Resolution*. Typical *Marion Dufresne* cores of 30 to 40 m length might contain deep samples with lower pore water SO_4^{2-} and higher gas concentrations. With more gas, the carbon isotopic composition could be determined. Clearly, deep coring of the type carried out by ODP would enable the BSR to be penetrated, and the overlying sediments to be directly examined for gas hydrates.

9. ACKNOWLEDGEMENTS

We sincerely thank the crew of the *RV L'Atalante* for an enjoyable and successful cruise. Gérald Beneton, Caroline François, Fabien Juffroy, Alexandre Leroy, Sabrina Van de Beuque and Olivier Voutay helped our efforts on the ship. Charles Paull and Bill Ussler at MBARI are thanked for use of their pore water squeezers. We thank the technicians in the Marine and Freshwater Research Group at JCU for sulphate and chloride analyses. AGSO isotope and organic geochemistry staff, Zoltan Horvath and Janet Hope, are thanked for the gas and extract analyses. Barry Willcox and Melissa Fellows of AGSO reviewed this publication. The members of IMB Graphic Services team in AGSO are thanked for drafting many of the figures and preparing the PDF version of this Record.

10. REFERENCES

Adkins, J.F., Boyle, E.A., Keigwin, L. & Cortijo, E., 1997. Variability of the North Atlantic thermohaline circulation during the last interglacial period. *Nature*, 390: 154-156.

Auzende, J-M., Beneton, G., Dickens, G., Exon, N., Francois, C., Holdway, D., Juffroy, F., Lafoy, A., Leroy, A., Van de Beuque, S. & Voutay, O., 2000a. Mise en évidence de diapirs mésozoiques sur la bordure orientale de la ride de Lord Howe (Sud-Ouest Pacifique: campagne ZoNeCo 5. *Comptes Rendus Academie Science, Paris, Sciences de la Terre et des Planètes*, 330: 209-215.

Auzende J.-M., Bonnin, J., Olivet, J.-L., Pautot, G. & Mauffret, A. , 1971. An upper-Miocene salt layer in the western mediterranean basin. *Nature*, 230: 82-84.

Auzende, J-M., Beneton, G., Dickens, G., Exon, N., François, C., Holdway, D., Juffrois, F., Lafoy, Y., Leroy, Y., Van de Beuque, S. & Voutay, O., 2000a. Mise en évidence de diapirs mésozoïques sur la bordure orientale de la ride de Lord Howe (Sud-Ouest Pacifique): campagne ZoNéCo 5. *Comptes Rendu Academie Sciences Paris, Sciences de la Terre et des planètes* 330, 209-215

Auzende, J-M., Dickens, G.R., Van de Beuque, S., Exon, N.F., François, C., Lafoy, Y., & Voutay, O., 2000b. Thinned crust in southwest Pacific may harbor gas hydrate. *EOS*, Transactions of American Geophysical Union, 81(17): 182-185.

Baker, P.A., 1986. Pore-water chemistry of carbonate-rich sediments, Lord Howe Rise, Southwest Pacific Ocean. *Initial Reports of the Deep Sea Drilling Project*, 90: 1249-1256.

Bangs, N.L.B., Sawyer, D.S. & Golovchenko, X., 1993. Free gas at the base of the gas hydrate zone in the vicinity of the Chile Triple Junction. *Geology*, 21: 905-908.

Bloemendal, J., Lamb, B. & King, J., 1988. Palaeoenvironmental implications of rock magnetic properties of late Quaternary sediment cores from the Eastern Equatorial Pacific. *Paleoceanography*, 3: 61-87.

Borowski, W.S., Paull, C.K. & Ussler III, W., 1999. Global and local variations of interstitial sulfate gradients in deep-water, continental margin sediments: Sensitivity to underlying methane and gas hydrates. *Marine Geology*, 159: 131-154.

Burns, R.E., Andrews, J.E. et al., 1973. *Initial Reports of the Deep Sea Drilling Project*, 21. U.S. Government Printing Office, Washington, D.C.

Cortijo, E., Yiou, P., Labeyrie, L. & Cremer, M., 1995. Sedimentary record of rapid climatic variability in the North Atlantic Ocean during the last glacial cycle. *Paleoceanography*, 10: 911-926.

Dickens, G.R., 2001. Sulfate profiles and barium fronts in sediment on the Blake Ridge: Present and past methane fluxes through a large gas hydrate reservoir. *Geochimica et Cosmochimica Acta*, 65: 529-543.

Dickens, G.R. & R.M. Owen, 1996. Sediment geochemical evidence for an early-middle Gilbert (early Pliocene) productivity peak in the North Pacific Red Clay Province. *Marine Micropaleontology*, 27: 107-120.

Dickens G.R., Paull, C.K., Wallace, P. & the ODP Leg 164 Scientific Party, 1997. Direct measurement of *in situ* methane quantities in a large gas hydrate reservoir. *Nature*, 385: 426-428.

Dickens, G.R. & Quinby-Hunt, M.S. 1994. Methane hydrate stability in seawater. *Geophysical Research Letters*, 21: 2115-2118.

Dickens, G.R., Snoeckx, H. Arnold, E., Morley, J.J., Owen, R.M., Rea, D.K. & Ingram, B.L., 1995. Composite depth scale and stratigraphy for Sites 885/886. *Proceedings ODP, Scientific Reports*, 145: 205-217.

Dunbar, G.B., Dickens G.R. & Carter, R.M., 2000. Sediment flux across the Great Barrier Reef Shelf to the Queensland Trough over the last 300 k.y. *Sedimentary Geology*, 133: 49-92.

Exon, N.F., Dickens, G.R., Auzende, J.M., Lafoy, Y., Symonds, P.A. & van de Beuque, S., 1998. Gas hydrates and free gas on the Lord Howe Rise, Tasman Sea. *PESA* (Petroleum Exploration Society of Australia) *Journal*, 26, 148-158.

Exon, N.F., Hill, P.J., Dickens, G. & Lafoy, Y., 2001. R.V. *Franklin* FAUST 3 Cruise FR9/01: geophysics, geochemistry and sedimentology associated with a large inferred gas hydrate deposit, eastern Lord Howe Rise, Tasman Sea. *Pre-cruise summary prepared for Franklin operations group* (unpublished).

Fossing, H., Ferdelman, T.G. & Berg, P., 2000. Sulfate reduction and methane oxidation in continental margin sediments influenced by irrigation (South-East Atlantic off Namibia). *Geochimica Cosmochimica Acta*, 64: 897-910.

Froelich, P.M., Klinkhammer, G.P., Bender, M.L., Luedtke, N.A., Heath, G.R., Cullen, D. & Dauphin, P., 1979. Early oxidation of organic matter in pelagic sediments of the eastern equatorial Atlantic: Suboxic diagenesis. *Geochimica Cosmochimica Acta*, 43: 1075-1090.

Gaina, C., Muller, D.T., Royer, J-Y., Stock, J., Hardebeck & Symonds, P., 1998. The tectonic history of the Tasman Sea: a puzzle with 13 pieces. *Journal of Geophysical Research*, 103: 12413-12433

Gardner, J.V., Nelson, C.S. & Baker, P.A., 1986. Distribution and character of pale green laminae in sediment from Lord Howe Rise: a probable Late Neogene and Quaternary tephrostratigraphic record. *Initial Reports of the Deep Sea Drilling Project*. Washington, U.S. Government Printing Office 90, p. 1145-1159.

Hayes, D.E. & Ringis, J., 1973. Seafloor spreading in the Tasman Sea. *Nature*, 243: 454-458.

Heath, R.A., 1985. A review of the physical oceanography of the seas around New Zealand. *New Zealand Journal of Marine and Freshwater Research*, 19: 79-124.

Hinz, K. et al., 1985. Geophysical, geological and geochemical studies on the Lord Howe Rise. *Bundesanstalt für Geowissenschaften und Rohstoffe Report*, 193 p.

Holdway, D., Radlinski, A., Exon, N., Auzende, J-M. & Van de Beuque, S., 2000. Continuous multi-spectral fluorescence and absorption spectroscopy for hydrocarbon detection in ocean waters: Fairway Basin, Lord Howe Rise. *Australian Geological Survey Organisation Record* 2000/35, 57 p.

Hunt, C.P., Moskowitz, B.M. & Banerjee, S.K., 1995. Magnetic Properties of Rocks and Minerals. In *Rock Physics and Phase Relations*: *A Handbook of Physical Constants*. (AGU Reference Shelf 3), 189-204.

Karlin, R. & Levi, S., 1983. Diagenesis of magnetic minerals in Recent hemipelagic sediments. *Nature*, 303: 327-330.

Kennett, J.P., von der Borch, et al., 1985. *Initial Reports of the Deep Sea Drilling Project*. Washington, U.S. Government Printing Office 90, 1517p.

Kennicutt II, M.C. and J.M. Brooks, Recognition of areas effected by petroleum seepage: northern Gulf of Mexico continental slope. *Geo-Marine Letters 10*, 221-224, 1990.

Lafoy, Y., Bernardel, G. and Van de Beuque, S., 1998a. Campagne de sismique multitraces entre la marge Est Australienne et le Sud de l'arc des Nouvelles-Hébrides, *Rapport de la campagne Rig-Seismic 206, Programme FAUST, Rapport ZoNéCo*, 40 p.

Lafoy, Y., Van de Beuque, S., Bernardel, G., Missegue, F., Nercissian, A., Auzende, J-M., Symonds, P. & Exon, N., 1998b. Scientists study deep geological structure between New Hebrides arc and eastern Australian margin. *Eos*, Transactions American Geophysical Union, 79(50), 613-614.

MacKay, M.E., Jarrard, R.D., Westbrook, G.K., Hyndman, R.D. & Shipboard Scientific Party of Ocean Drilling Program Leg 146, 1994. Origin of bottom simulating reflectors: Geophysical evidence from the Cascadia accretionary prism. *Geology*, 22: 459-462.

Martínez, J.I., 1994. Late Pleistocene paleoceanography of the Tasman Sea: Implications for the dynamics of the warm pool in the western Pacific. *Palaeogeography Palaeoclimatology Palaeoecology*, 112: 19-62.

Morin, R.H., 1986. Physical properties of calcareous sediments from the southwest Pacific. *Initial Reports of the Deep Sea Drilling Project*, 90: 1239-1240.

Morin, R.H. & von Herzen, R.P., 1986. Geothermal measurements at Deep Sea Drilling Project Site 587. *Initial Reports of the Deep Sea Drilling Project*, 90: 1317-1324.

Mix, A.C., Harris, S.E. and Janecek, T.R., 1995. Estimating lithology from nonintrusive reflectance spectra: Leg 138. *Proceedings of the Ocean Drilling Program, Scientific Results*, 138: 413-428.

Mulhearn, P.J., 1987. The Tasman Front: A study using satellite infrared imagery. *Journal of Physcial Oceanography*, 17(8): 1148-1155.

Paull, C.K., W. Ussler III, W.S. Borowski, and F.N. Speiss, 1995. Methane-rich plumes on the Carolina continental rise: Associations with gas hydrates. *Geology*, *23*, 89-92.

Pautot G., J.M. Auzende J-M. and Le Pichon X., 1970. Continuous deep-sea salt layer along North Atlantic margin related to early phase of rifting. *Nature*, 227, 351-354.

Robinson, S.G., 1993. Lithostratigraphic applications for magnetic susceptibility logging of deep-sea sediment cores: examples from ODP Leg 115. In Hailwood, E.A. & Kidd, R.B. (Eds), *High Resolution Stratigraphy*. Geological Society Special Publication, 70, 65-98.

Shipboard Scientific Party, 1986. Site 588: Lord Howe Rise, 26°S. Initial Reports of the Deep Sea Drilling Project, *Washington, U.S. Government Printing Office* 90, 139-252.

Taylor, M.H., Dillon, W.P. and Pecher, I.A., 2000. Trapping and migration of methane associated with the gas hydrate stability zone at the Blake Ridge diapir; new insights from seismic data. *Marine Geology*, 164, 79-89.

Thompson, R. & Oldfield, F., 1986. *Environmental magnetism*. Boston: Allen & Unwin, 227 p.

Thomson, J., Higgs, N.C., Croudace, I.W., Colley, S. & Hydes, D.J., 1993. Redox zonation of elements at an oxic/post-oxic boundary in deep-sea sediments. *Geochimica Cosmochimica Acta*, 57: 579-595.

Van de Beuque, S., Auzende, J-M., Lafoy, Y., Bernardel, G., Nercissian, A., Regnier, M., Symonds, P. & Exon, N., 1998. Transect sismique continu entre l'arc des nouvelles-hébrides et la marge orientale de l'Australie: program FAUST (French Australian Seismic Transect). *Comptes Rendu Academie Science Paris, Sciences de la terre et des planetes*, 327, 761-768.

Warren, B.A., 1970. General circulation in the South Pacific. In W. S. Wooster (Ed.), *Scientific Exploration of the South Pacific*. National Academy of Sciences, 33-49.

Weissel, J.K. and Hayes, D.E., 1977. Evolution of the Tasman Sea reappraised, *Earth Planetary Science Letters*, 36, 77-84.

Westbrook, G.K., Carson, B., Musgrave, R.J., *et al.*, 1994. *Proceedings of the Ocean Drilling Program, Initial Reports*, 146(Pt. 1). College Station, Texas (ODP), 611 pp.

Xu, W. & Ruppel, C., 1999. Predicting the occurrence, distribution, and evolution of methane gas hydrate in porous marine sediments. *Journal of Geophysical Research*, 104: 5081-5095.

Plates 1-13. Colour photographs of the thirteen *ZoNéCo 5* cores with records of greyscale and magnetic susceptibility (MS). Shipboard colour intervals and shore-based physical property intervals (PI-PIII) also are noted.

ZONÉCO 5
KG 01 (0.00 - 4.00 mbsf)

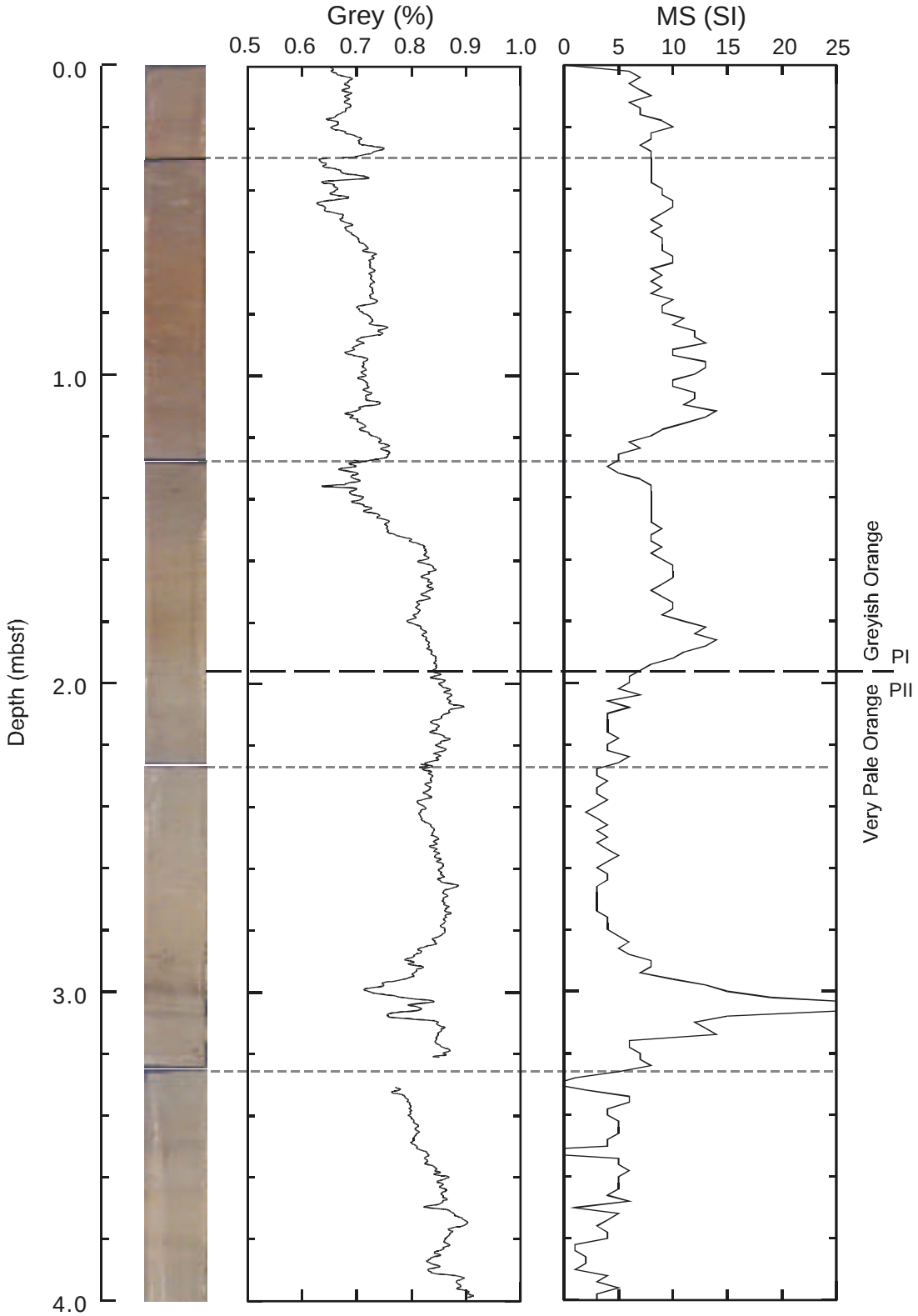

ZONÉCO 5
KG 01 (4.00 - 6.88 mbsf)

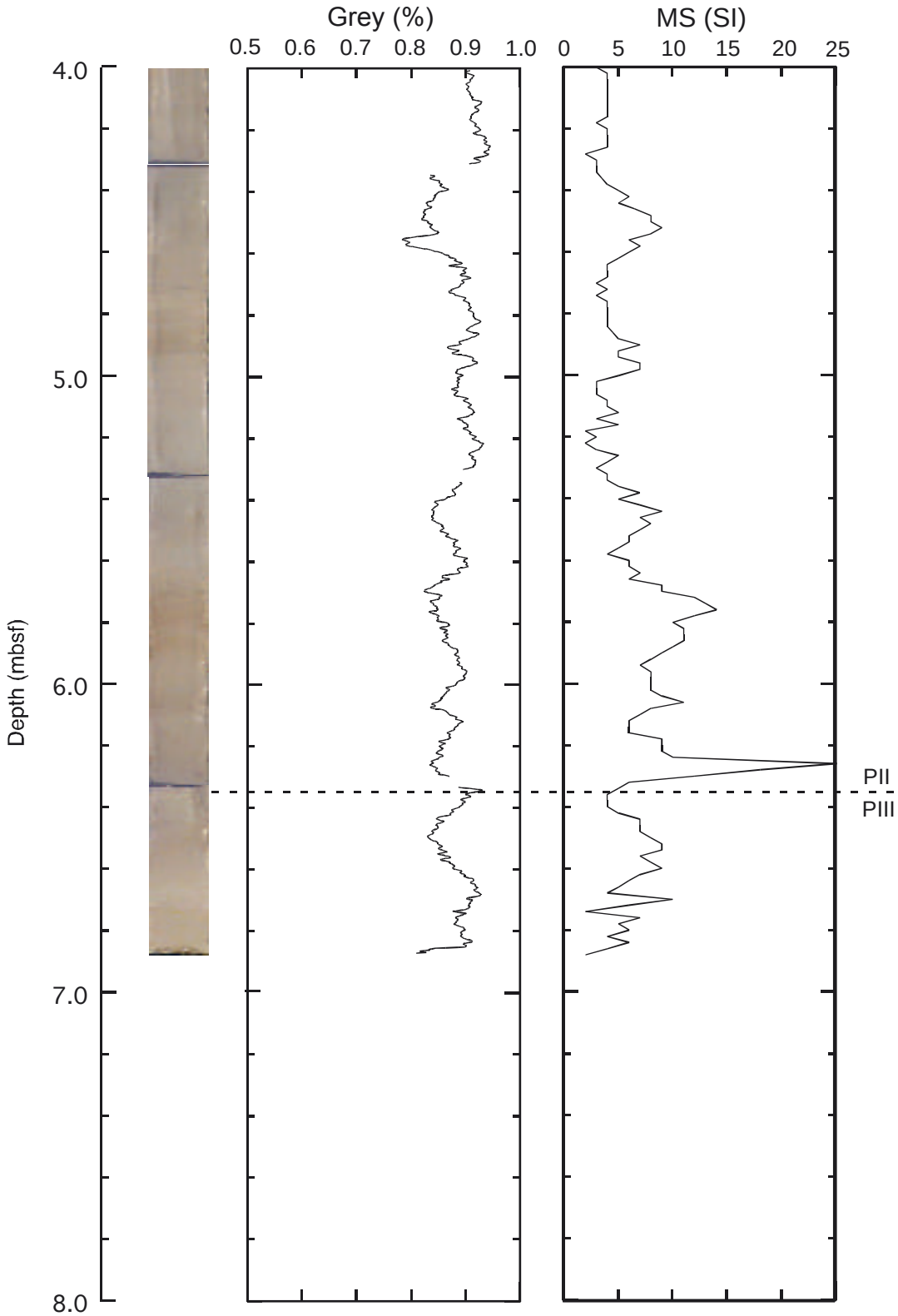

ZONÉCO 5
KG 02 (0.00 - 4.00 mbsf)

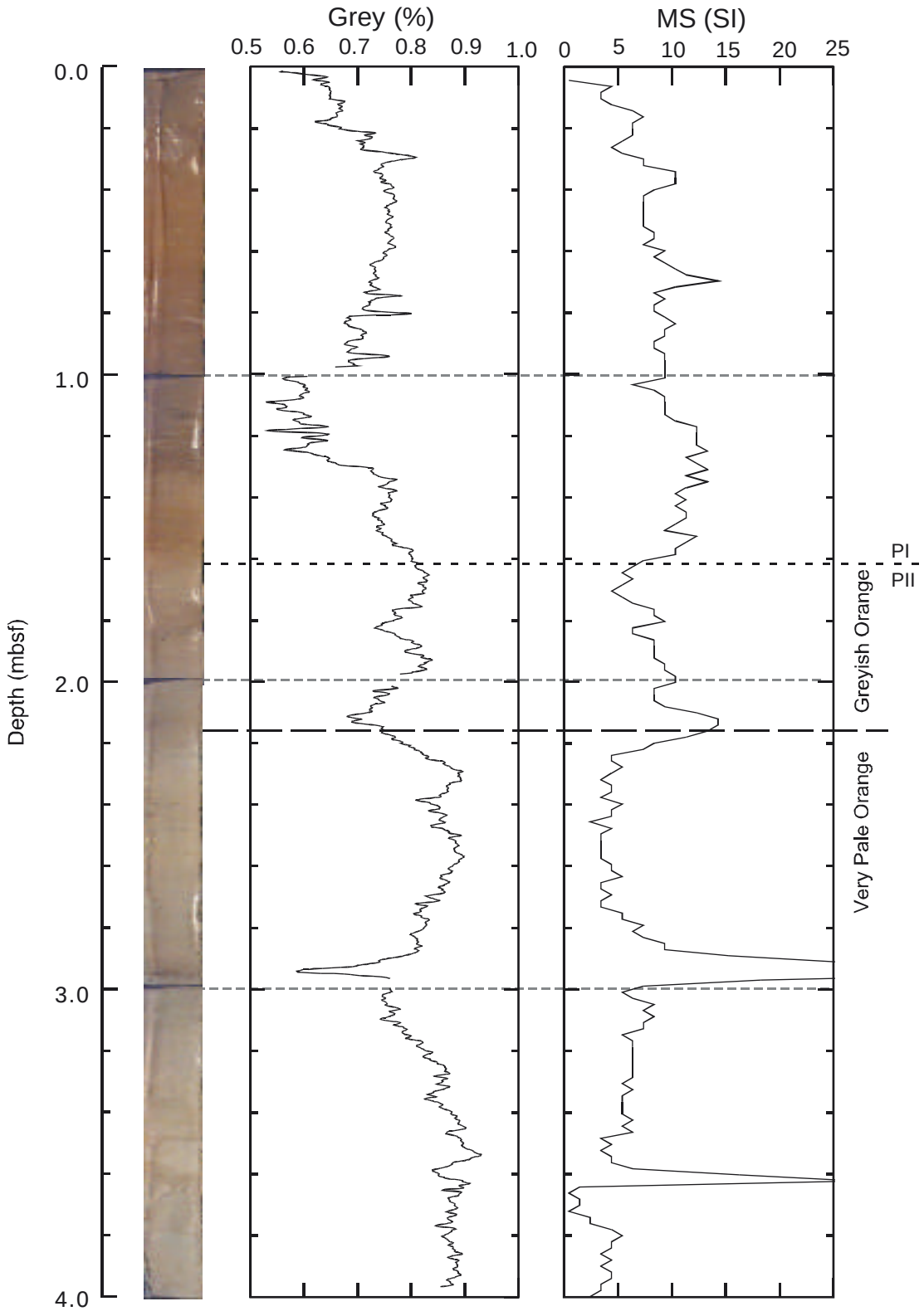

ZONÉCO 5

KG 02 (4.00 - 6.02 mbsf)

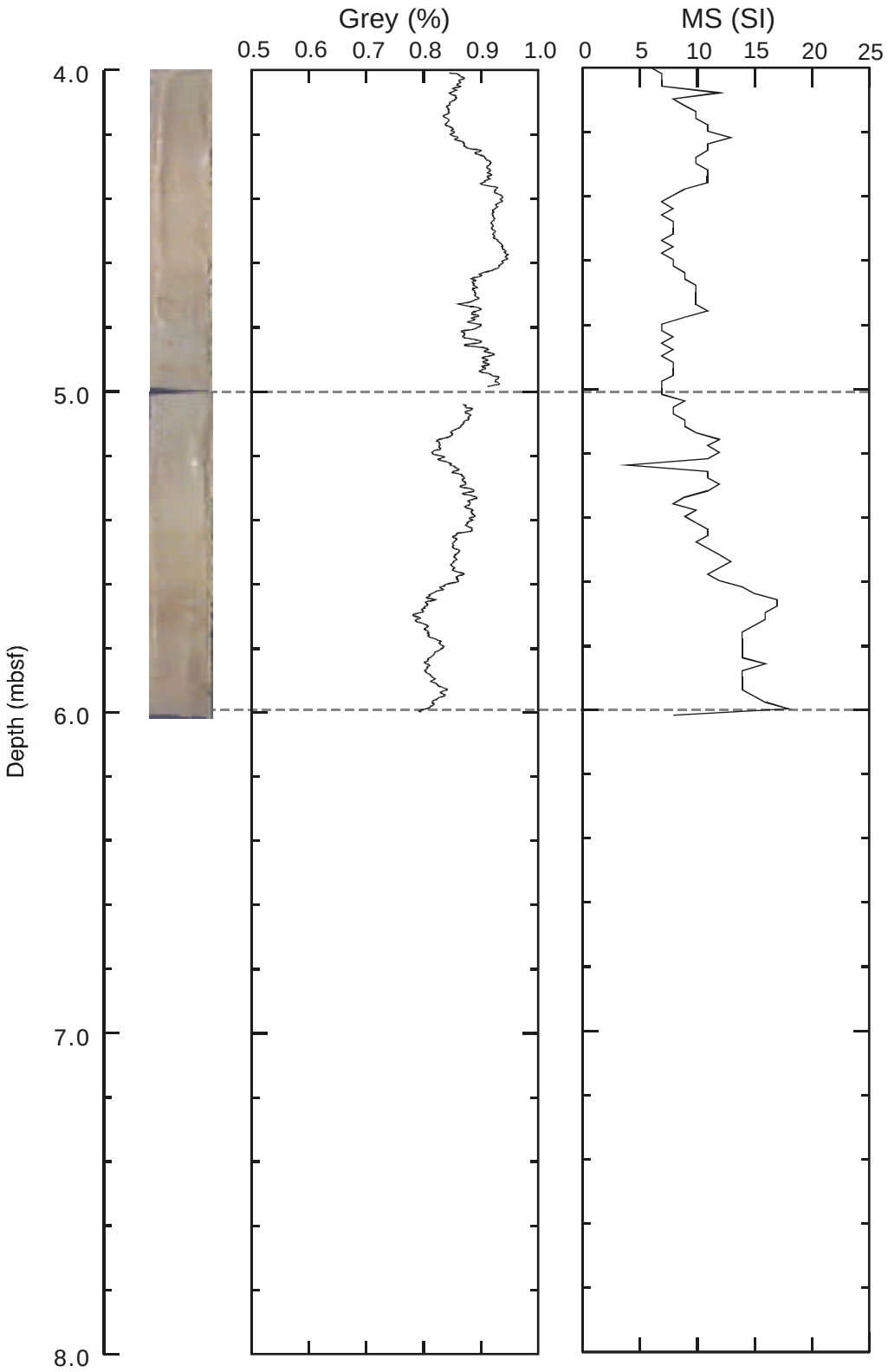

ZONÉCO 5
KG 03 (0.00 - 4.00 mbsf)

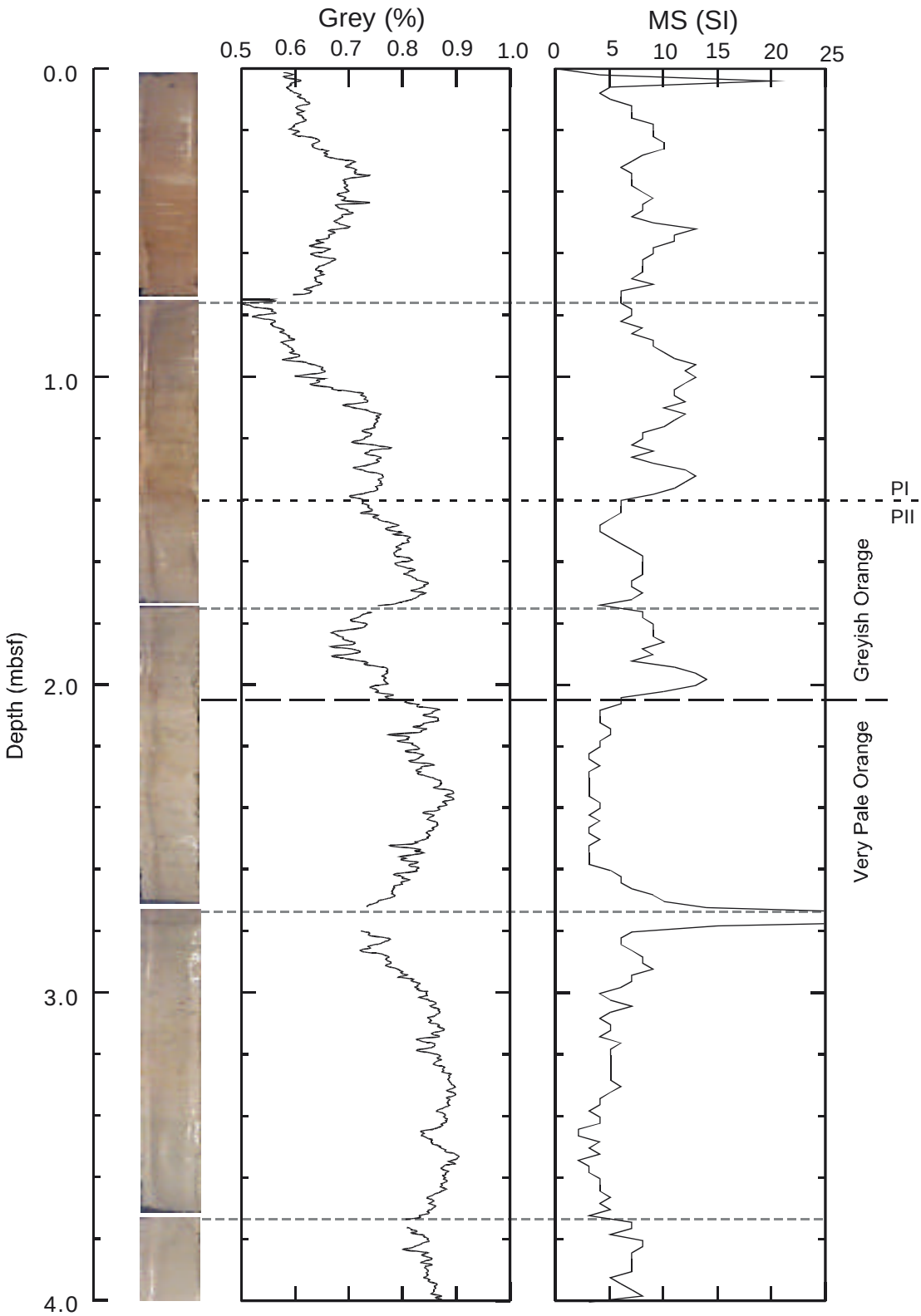

ZONÉCO 5
KG 03 (4.00 - 8.00 mbsf)

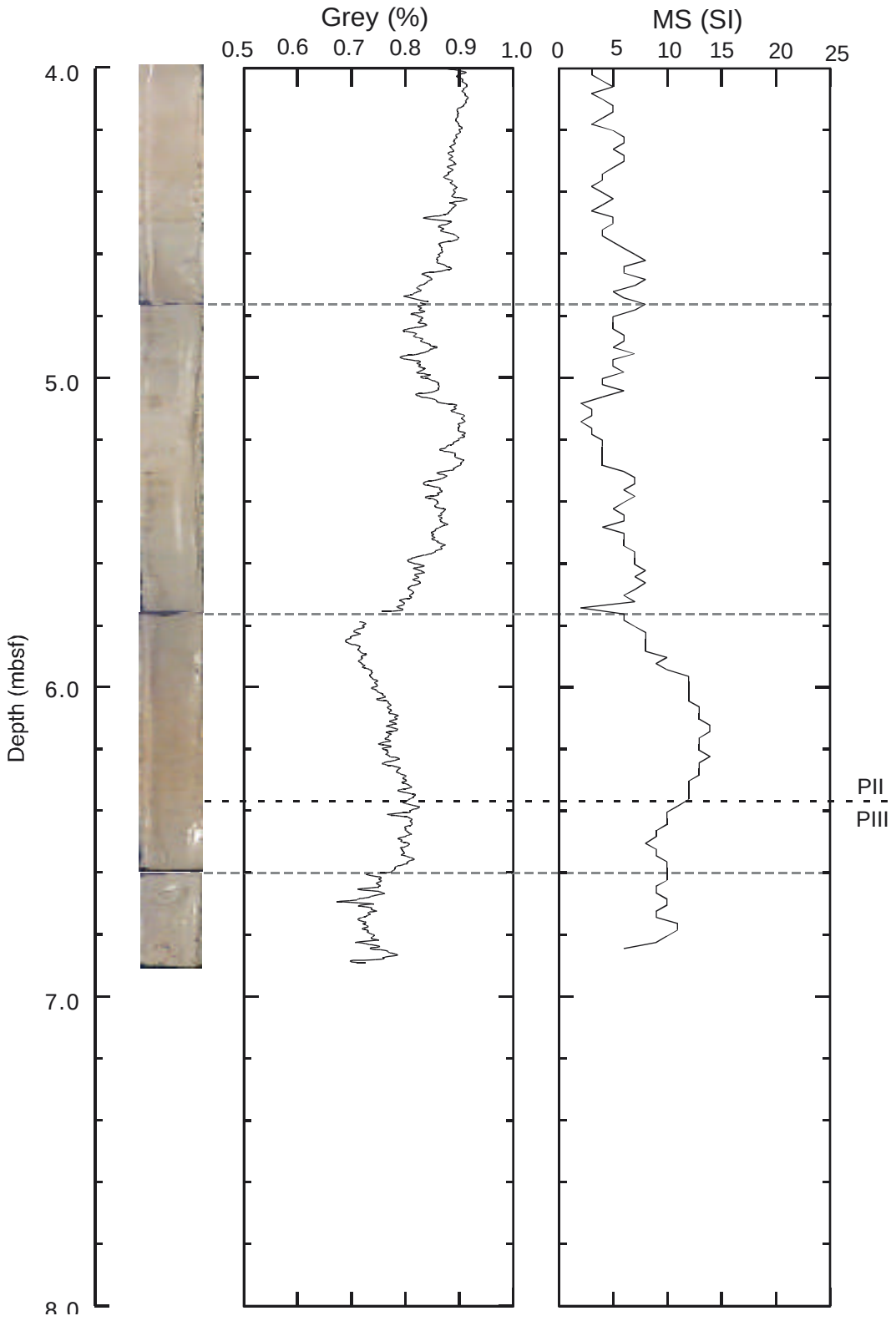

ZONÉCO 5
KG 04 (0.00 - 4.00 mbsf)

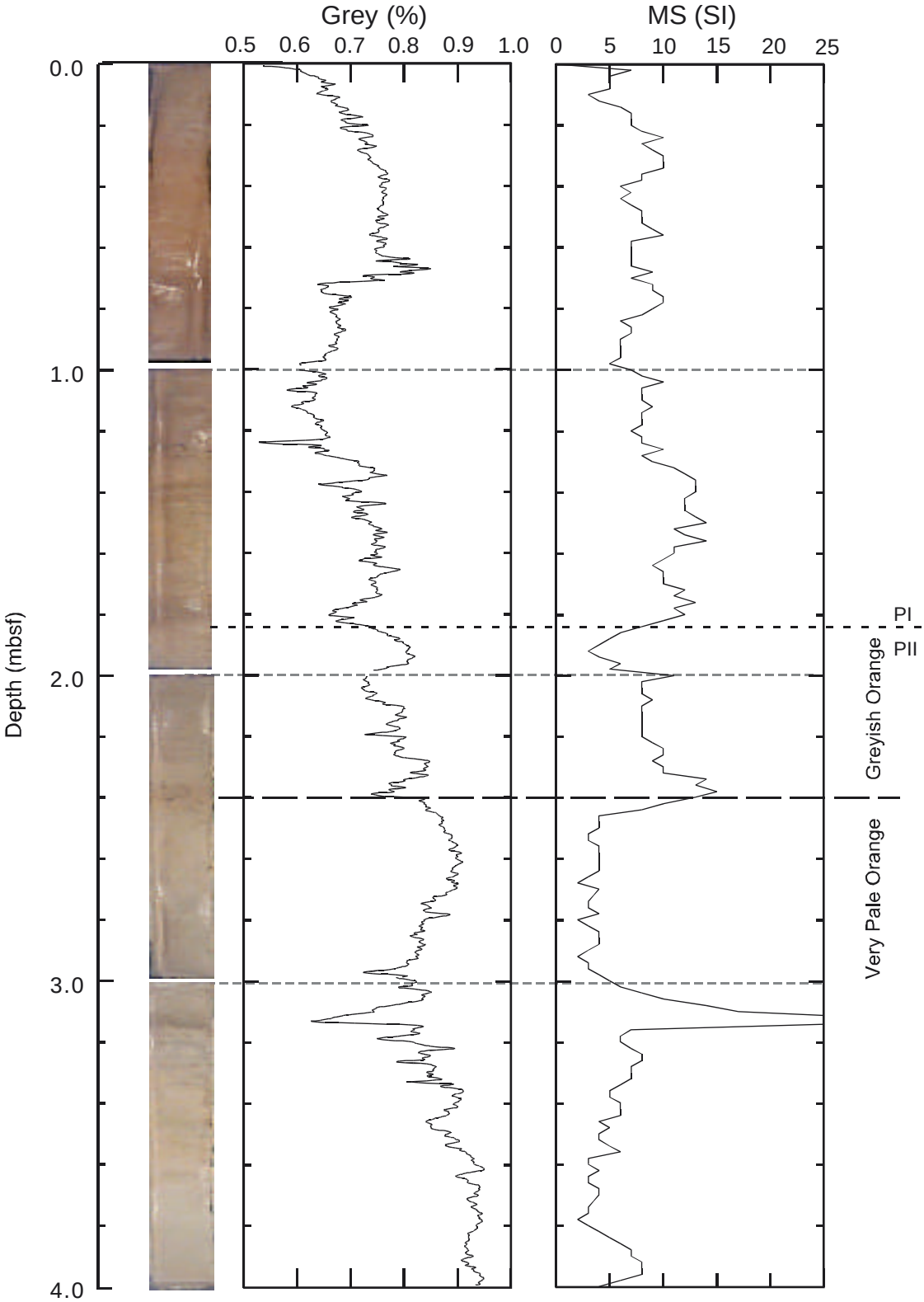

ZONÉCO 5
KG 04 (4.00 - 6.18 mbsf)

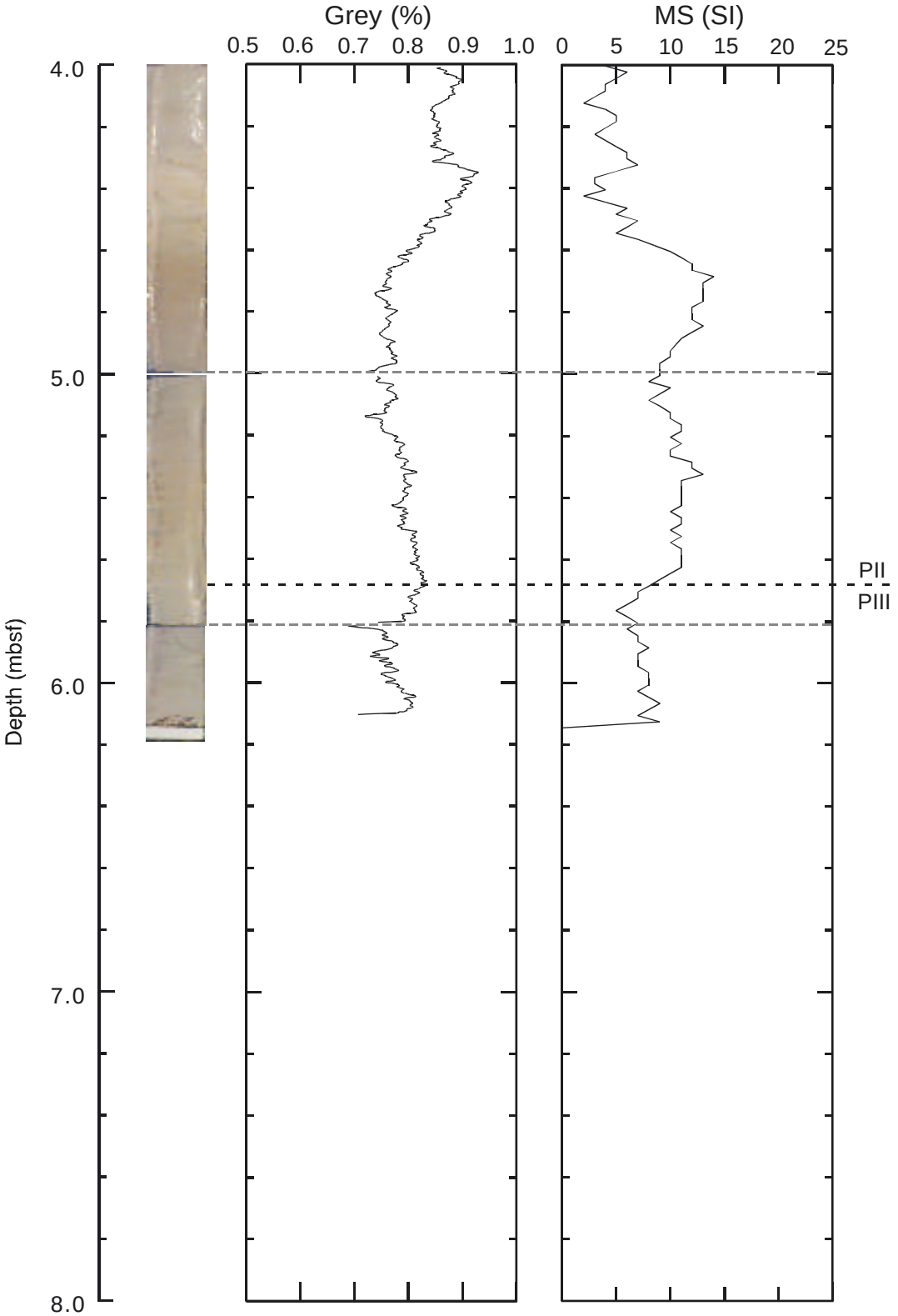

ZONÉCO 5
KG 05 (0.00 - 4.00 mbsf)

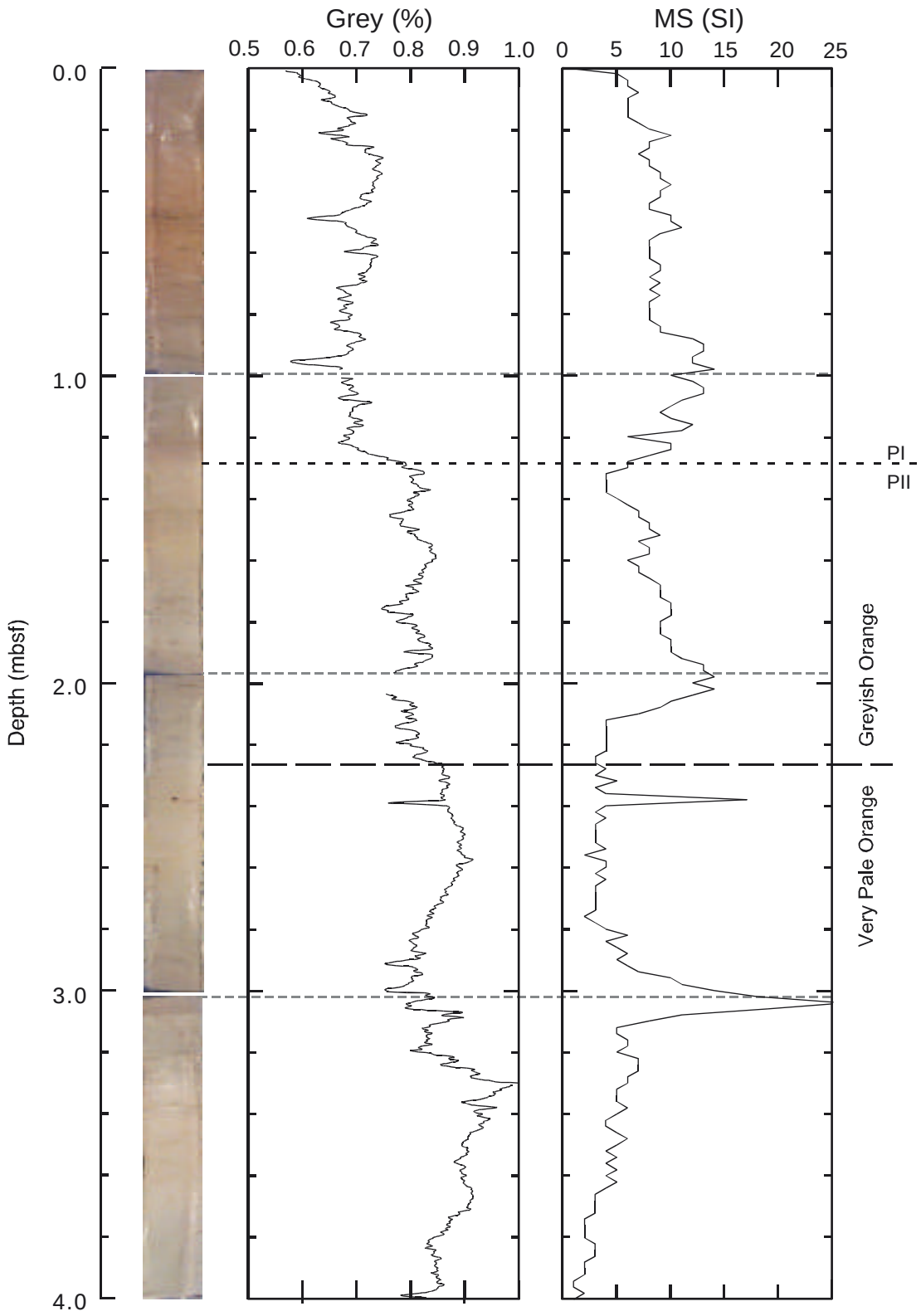

ZONÉCO 5
KG 05 (4.00 - 7.52 mbsf)

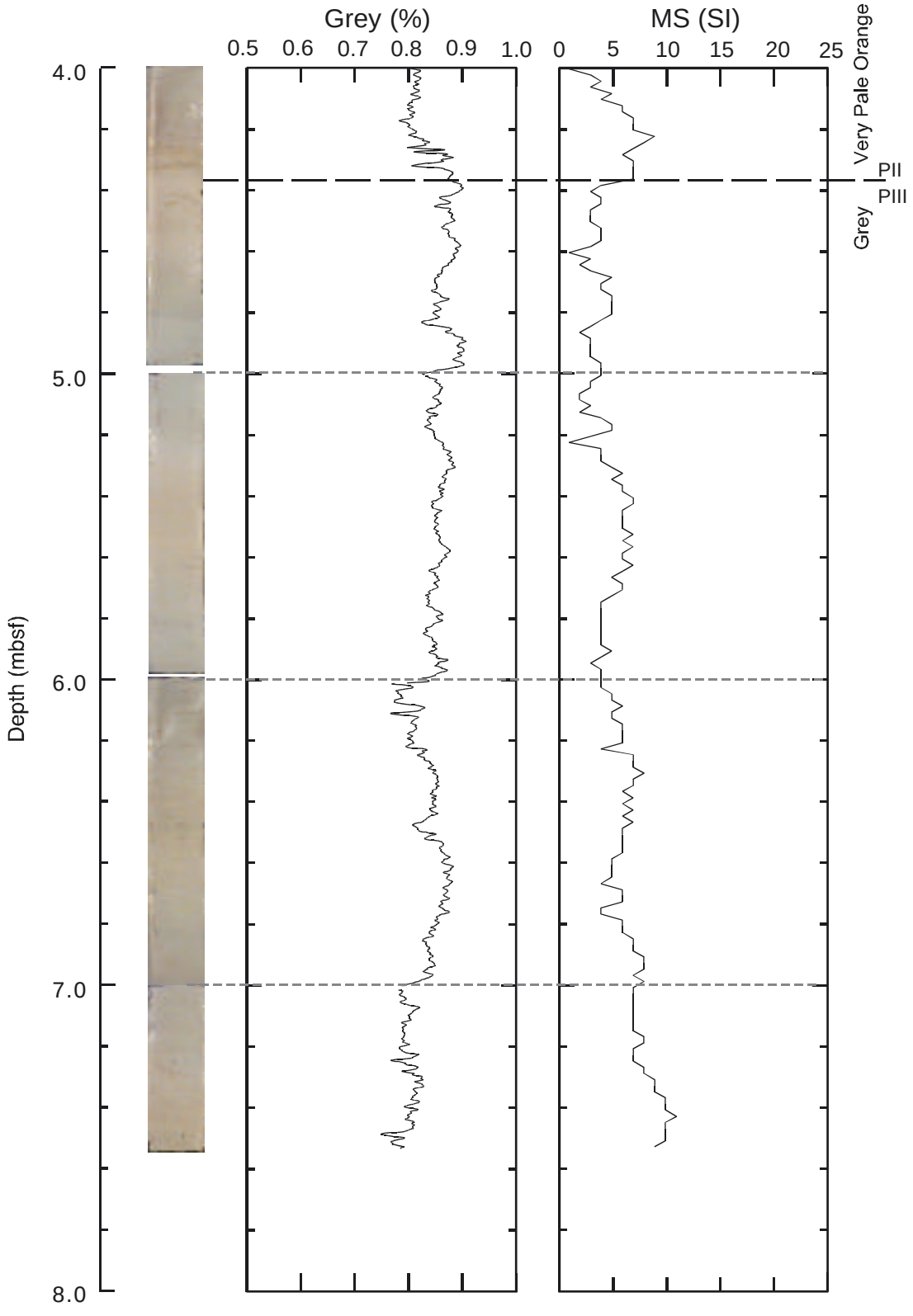

ZONÉCO 5
KG 06 (0.00 - 4.00 mbsf)

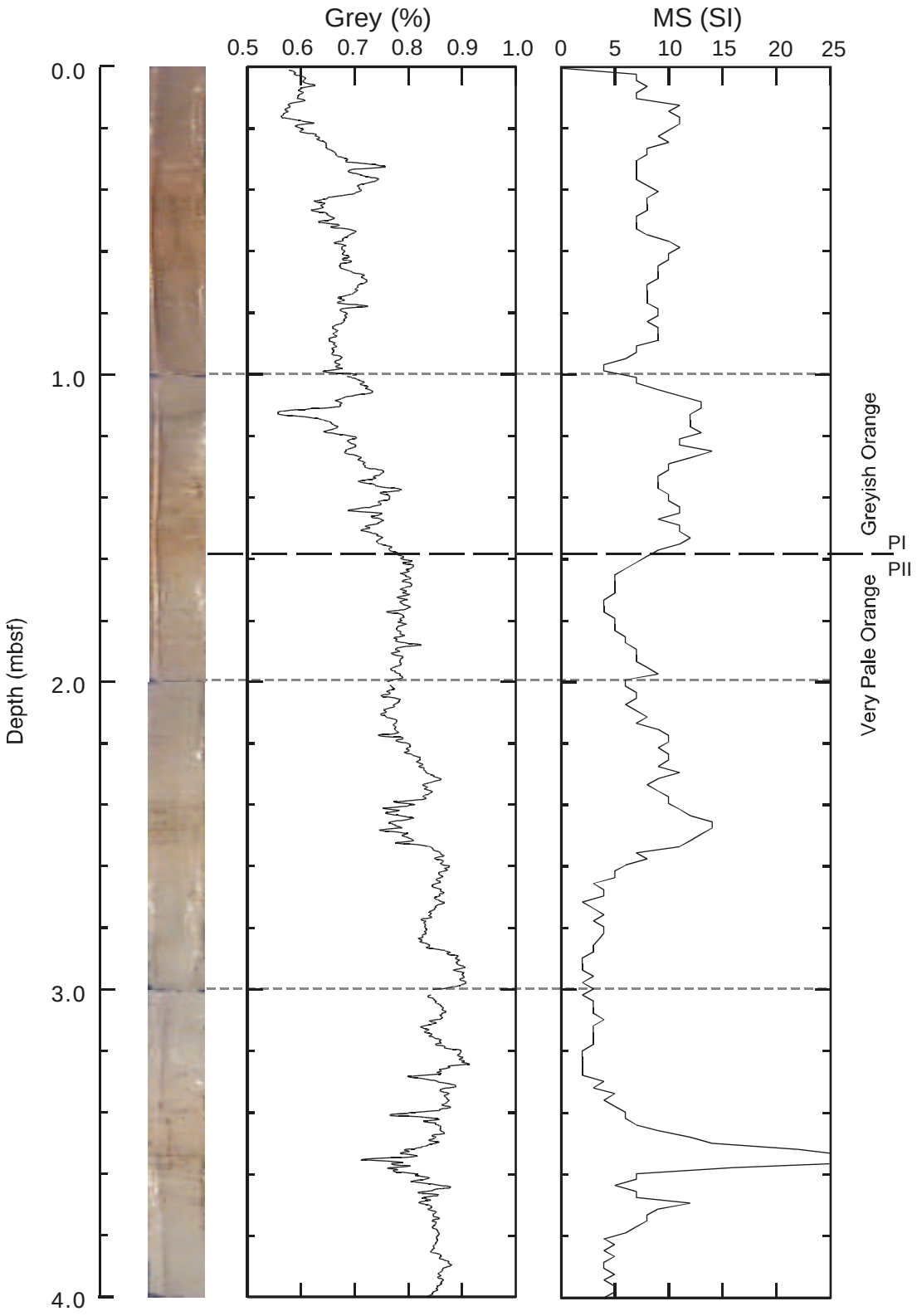

ZONÉCO 5
KG 06 (4.00 - 7.02 mbsf)

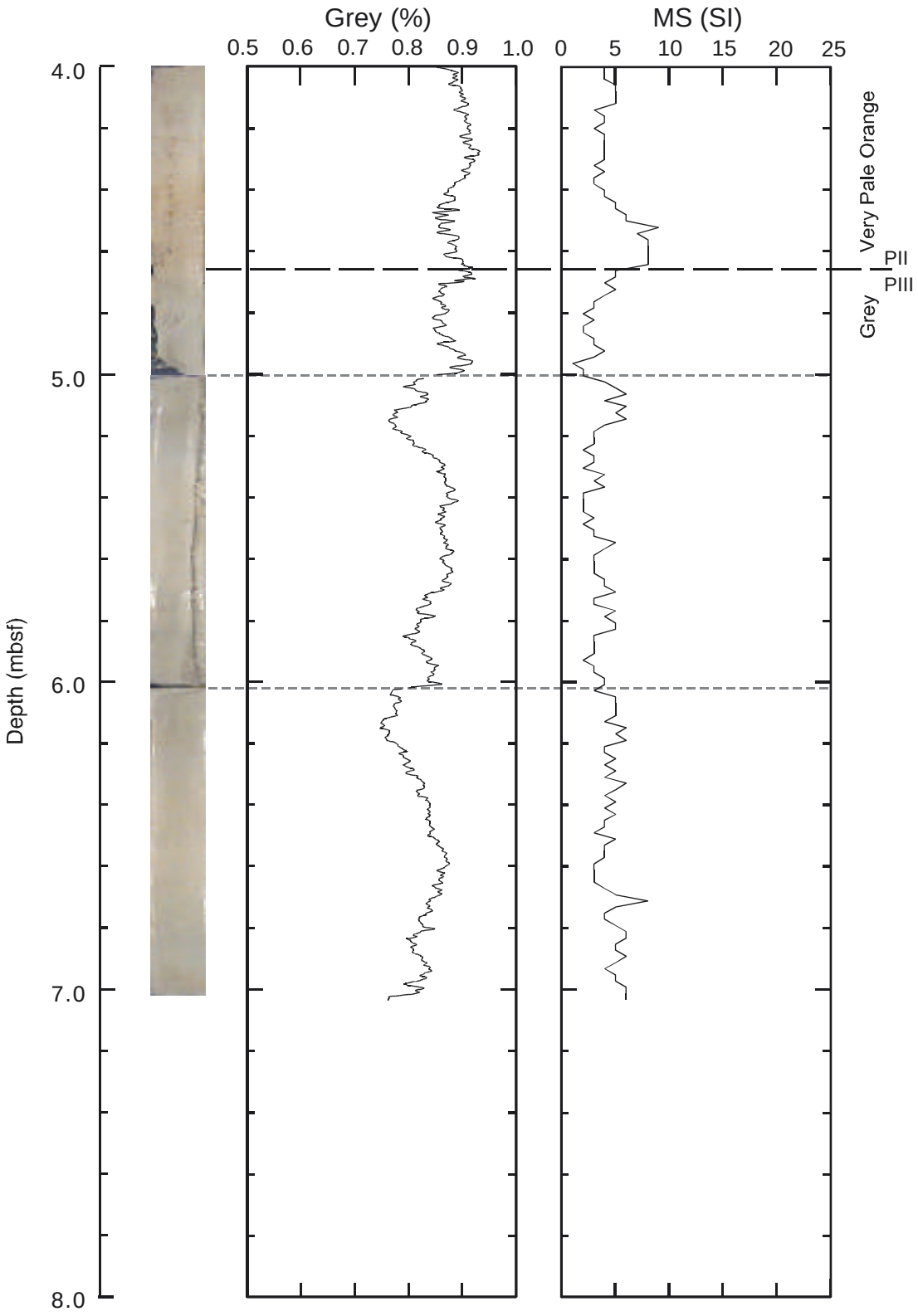

ZONÉCO 5
KG 07 (0.00 - 4.26 mbsf)

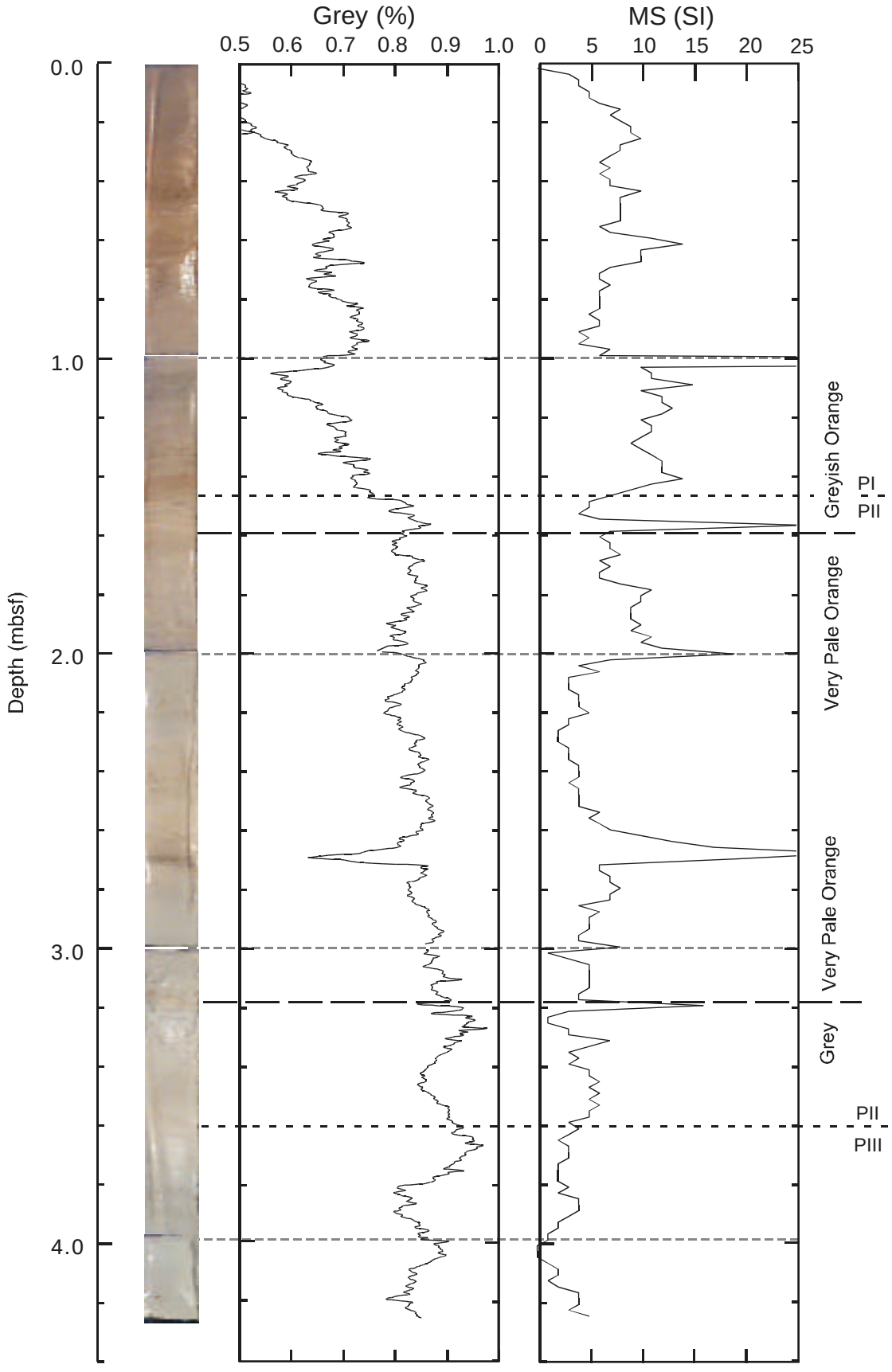

ZONÉCO 5
KG 08 (0.00 - 4.00 mbsf)

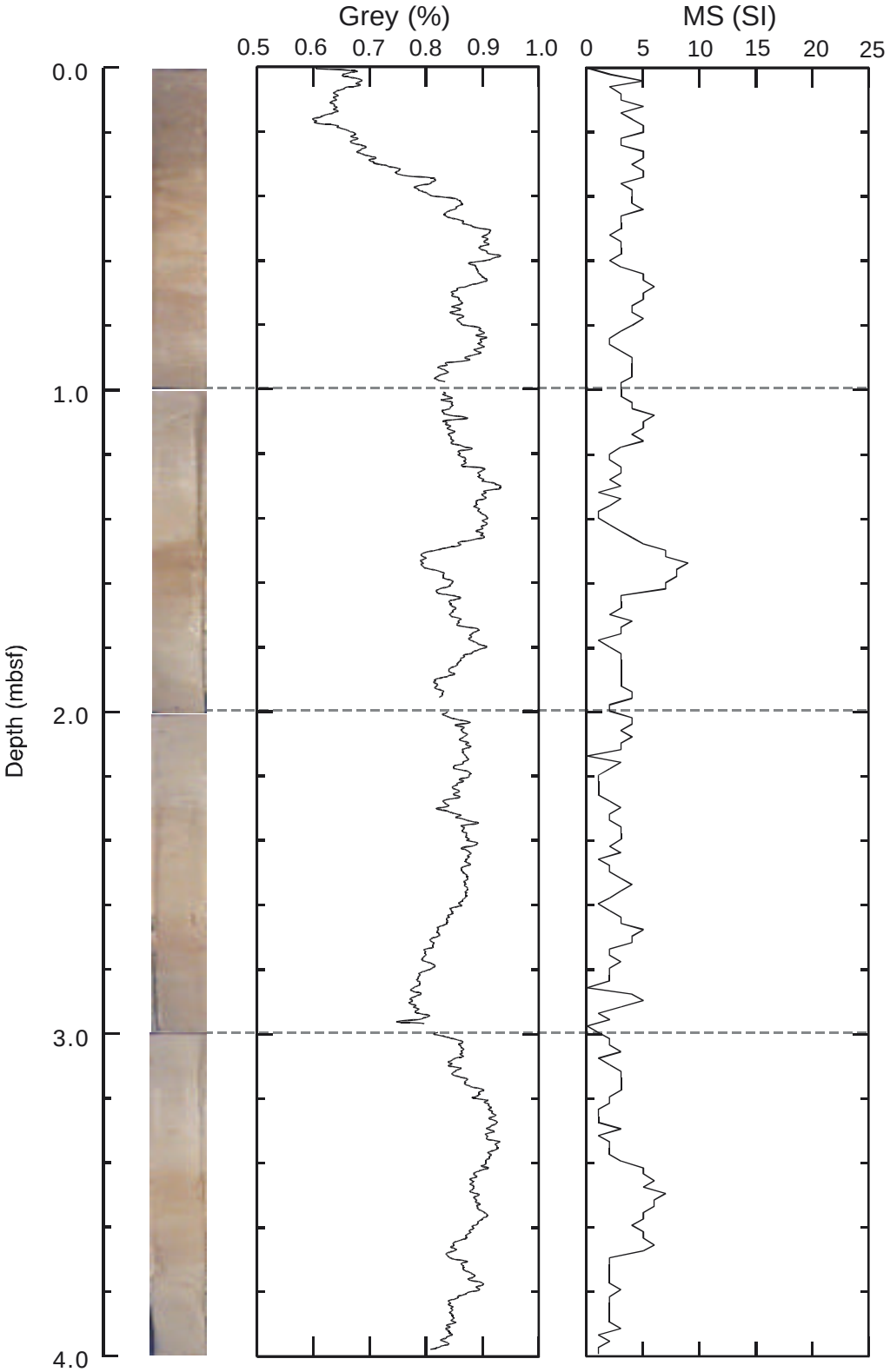

ZONÉCO 5
KG 08 (4.00 - 6.84 mbsf)

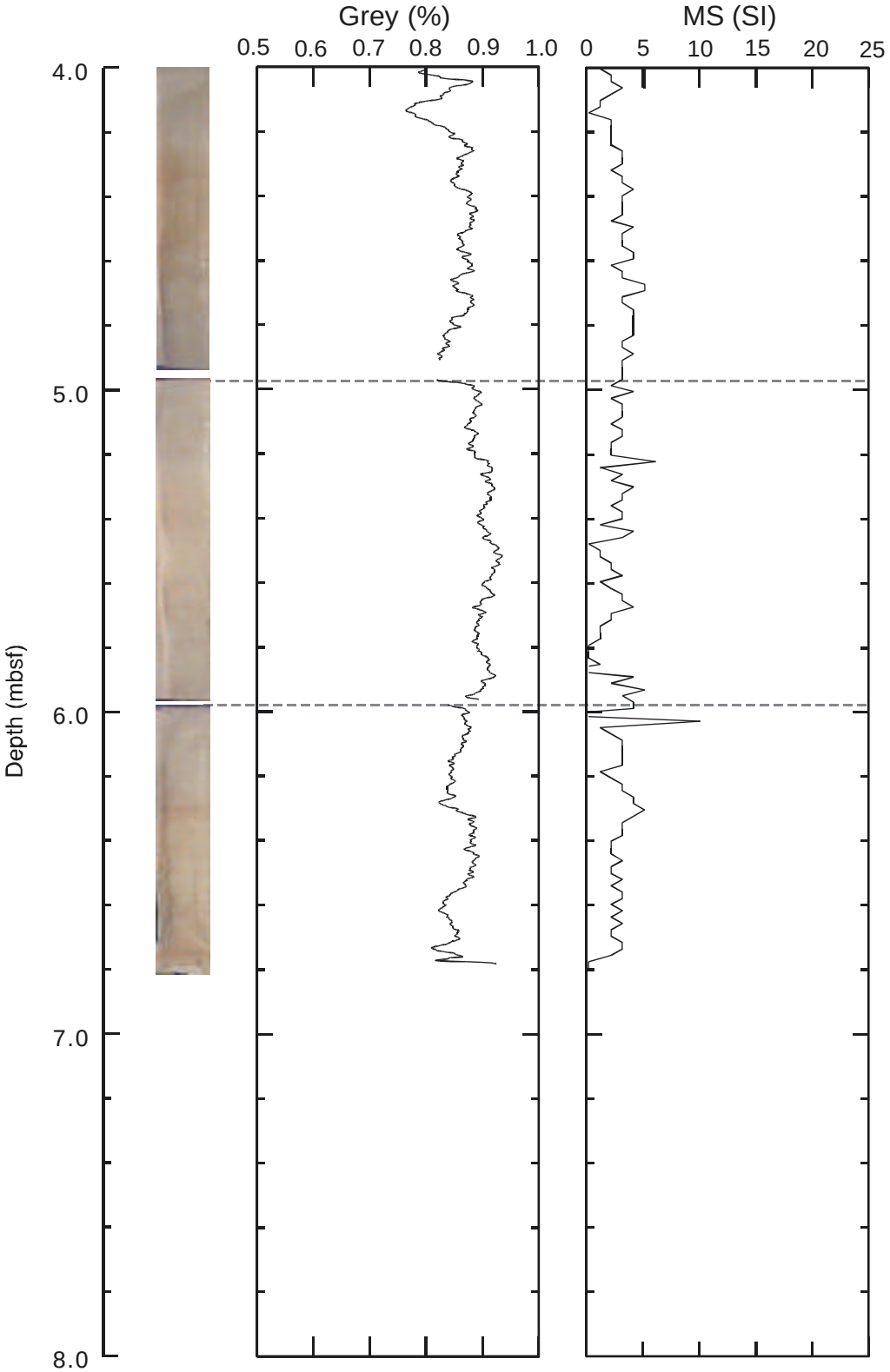

ZONÉCO 5
KG 09 (0.00 - 4.24 mbsf)

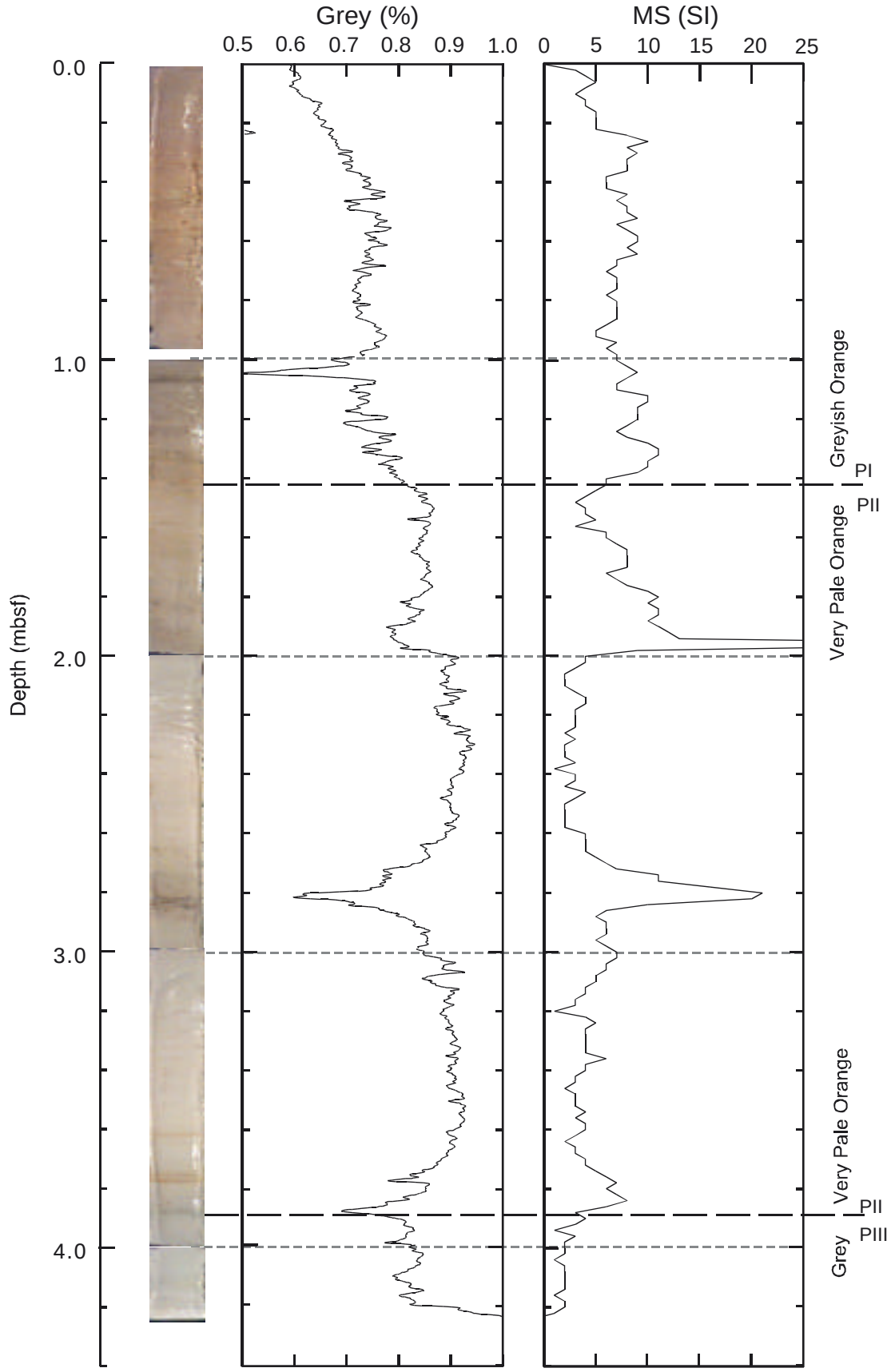

ZONÉCO 5
KG 10 (0.00 - 4.00 mbsf)

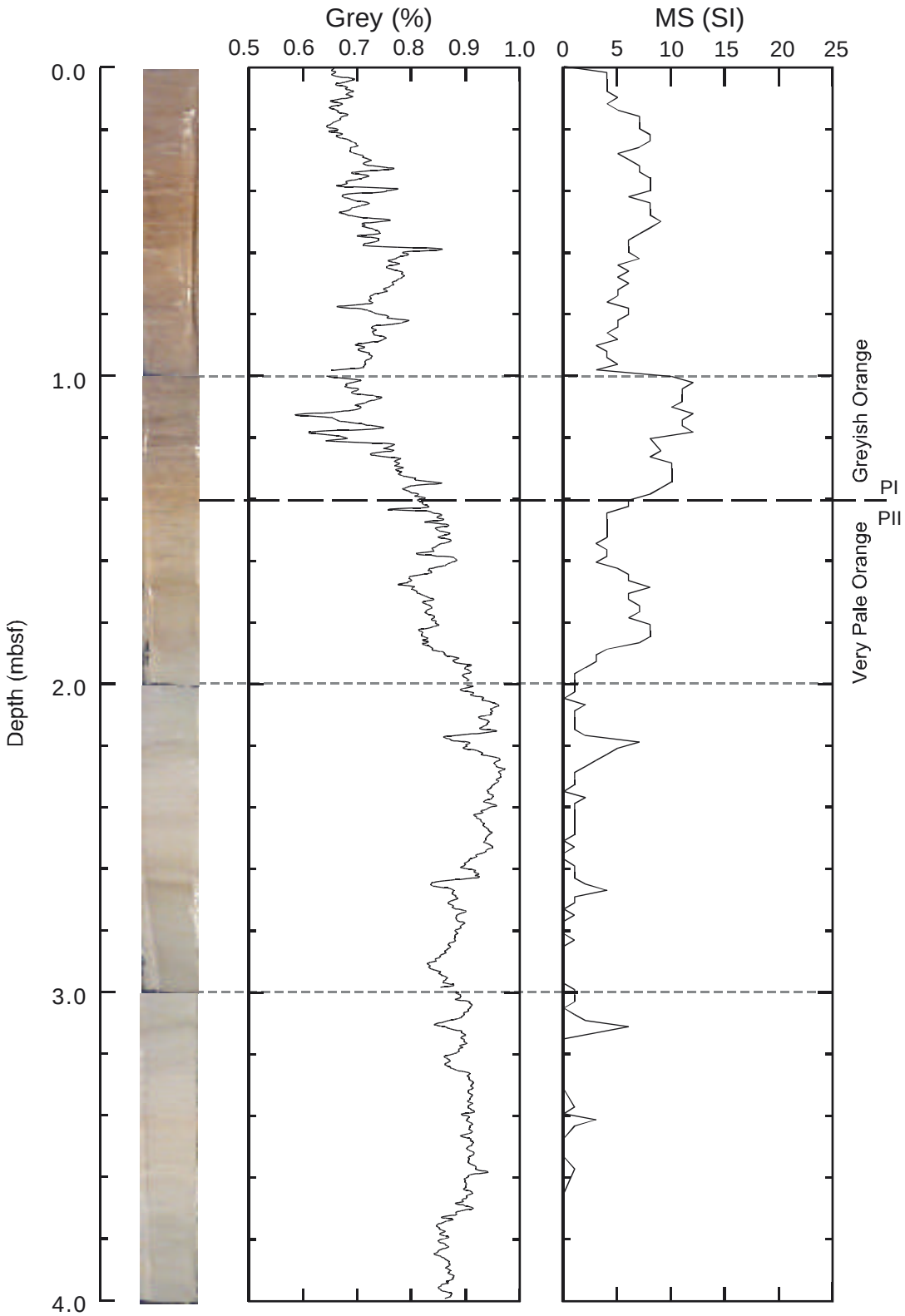

ZONÉCO 5
KG 10 (4.00 - 6.48 mbsf)

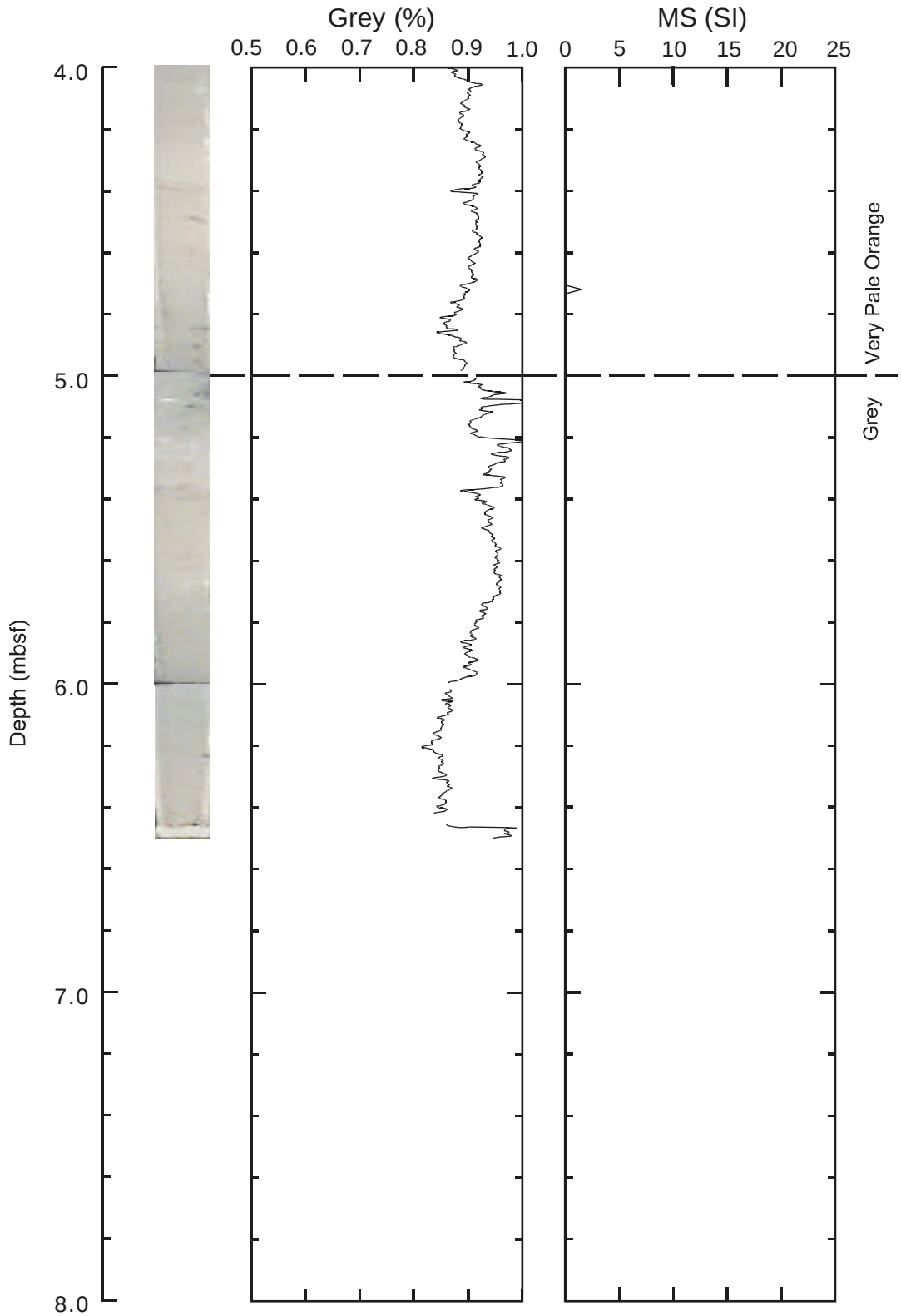

ZONÉCO 5
KG 11 (0.00 - 4.00 mbsf)

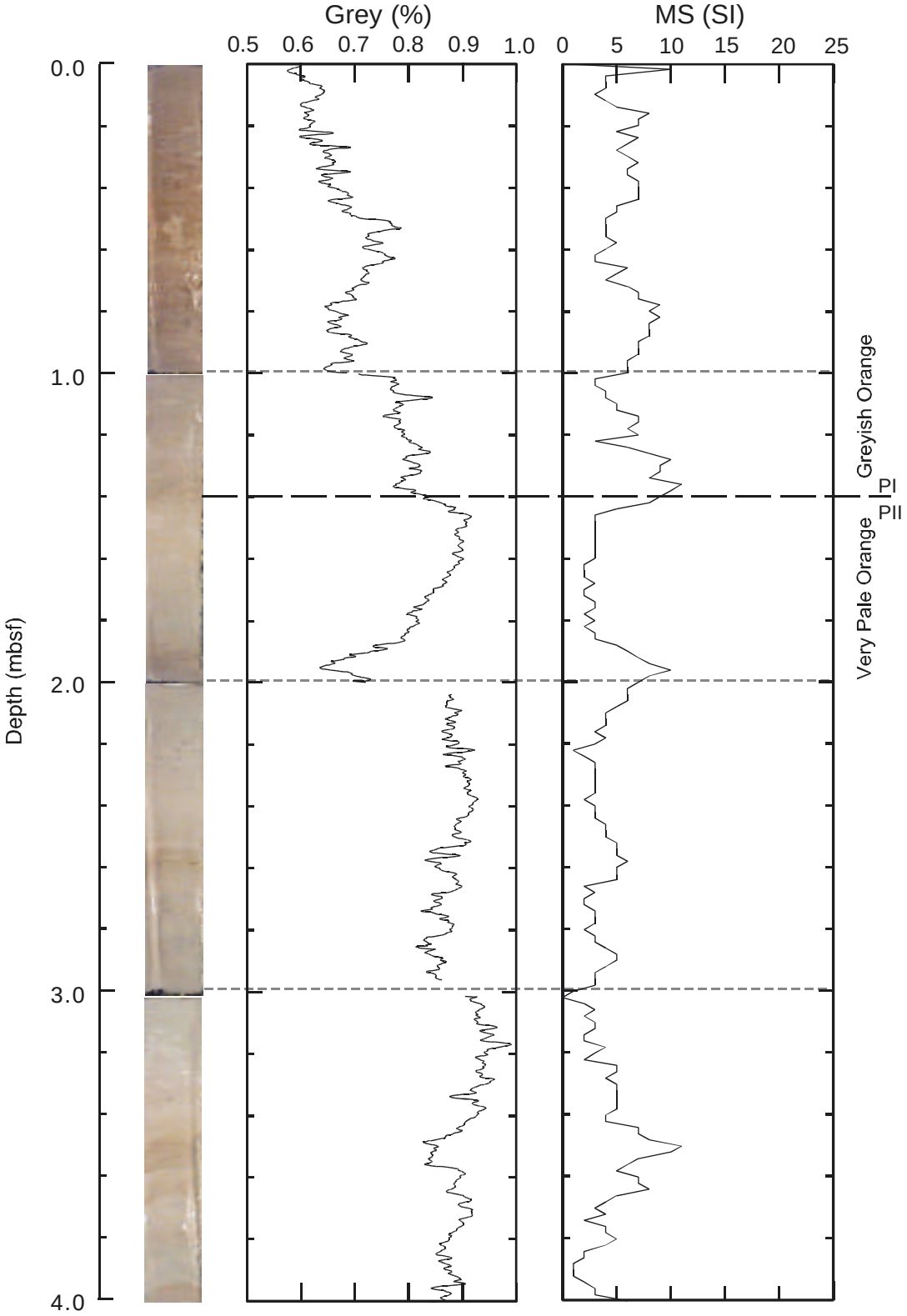

ZONÉCO 5
KG 11 (4.00 - 5.84 mbsf)

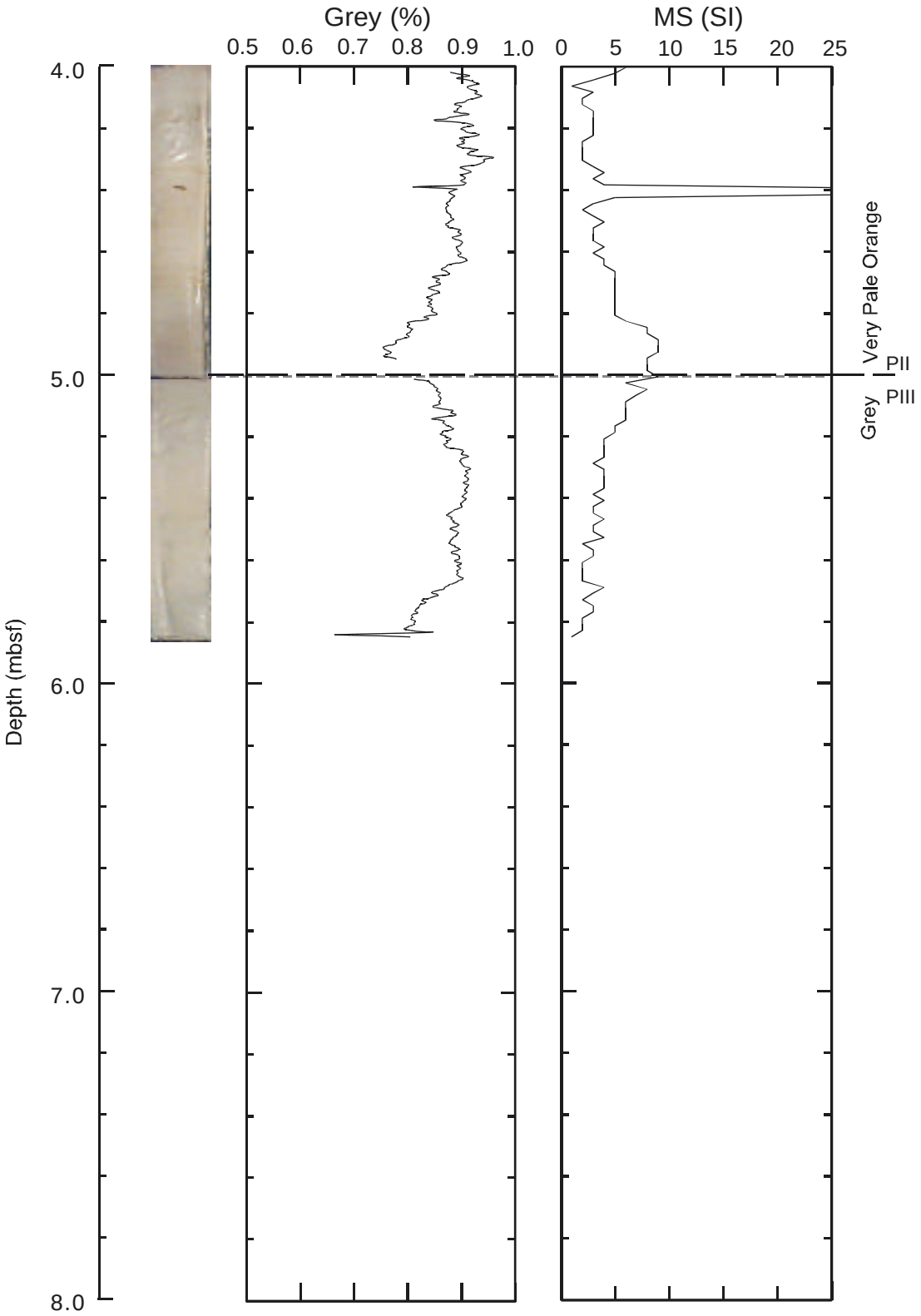

ZONÉCO 5
KG 12 (0.00 - 4.00 mbsf)

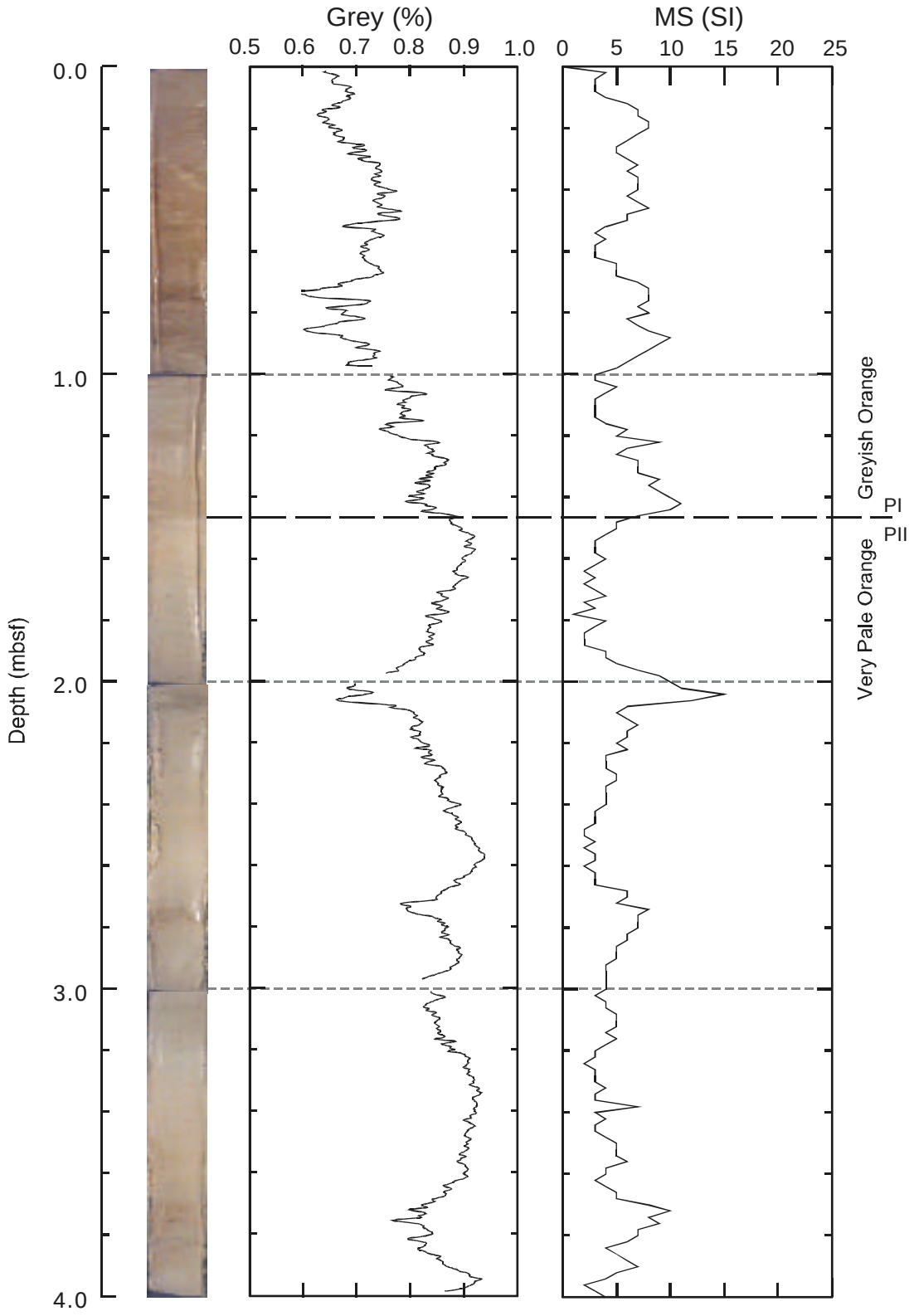

ZONÉCO 5
KG 12 (4.00 - 7.60 mbsf)

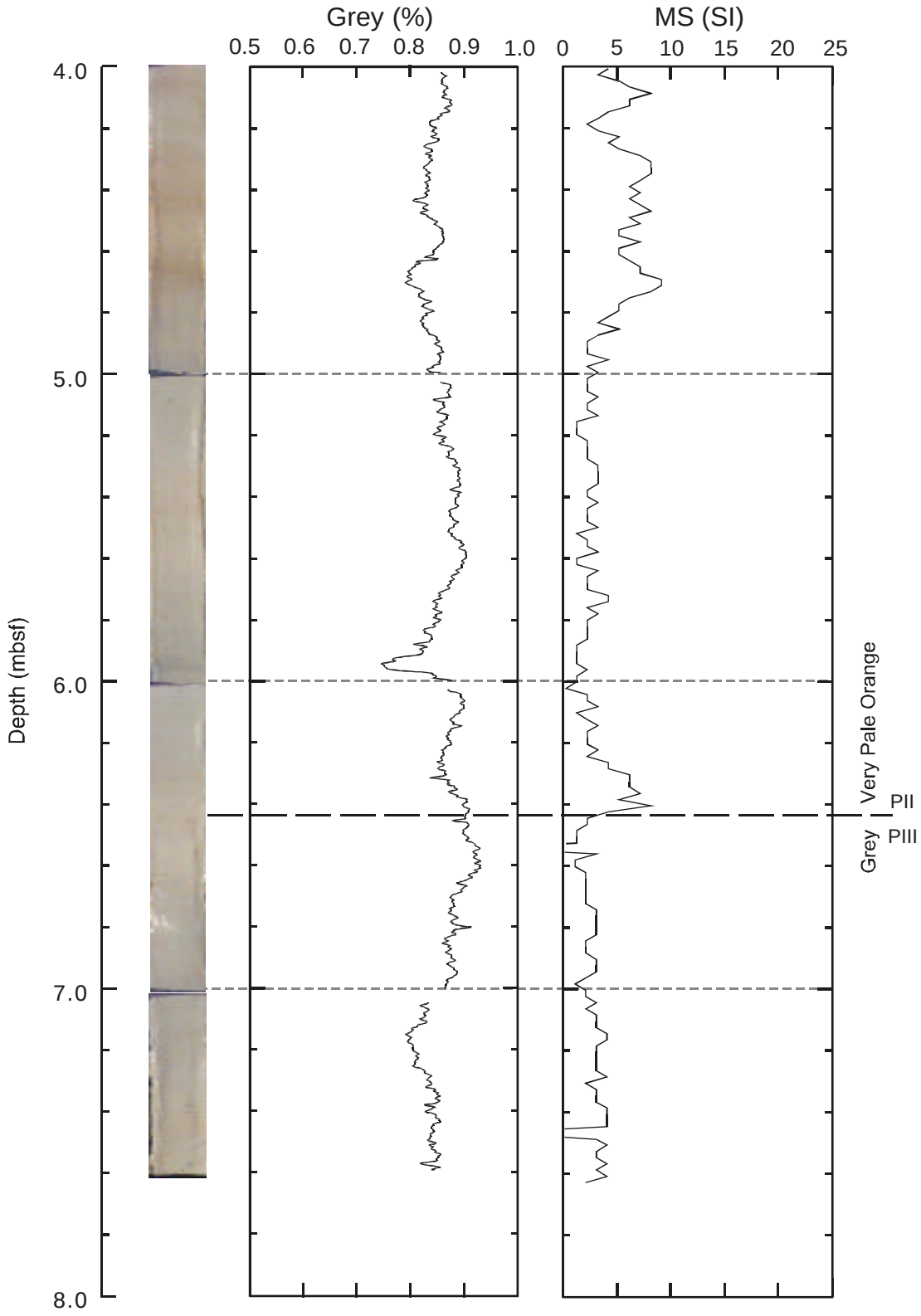

ZONÉCO 5
KG 13 (0.00 - 4.00 mbsf)

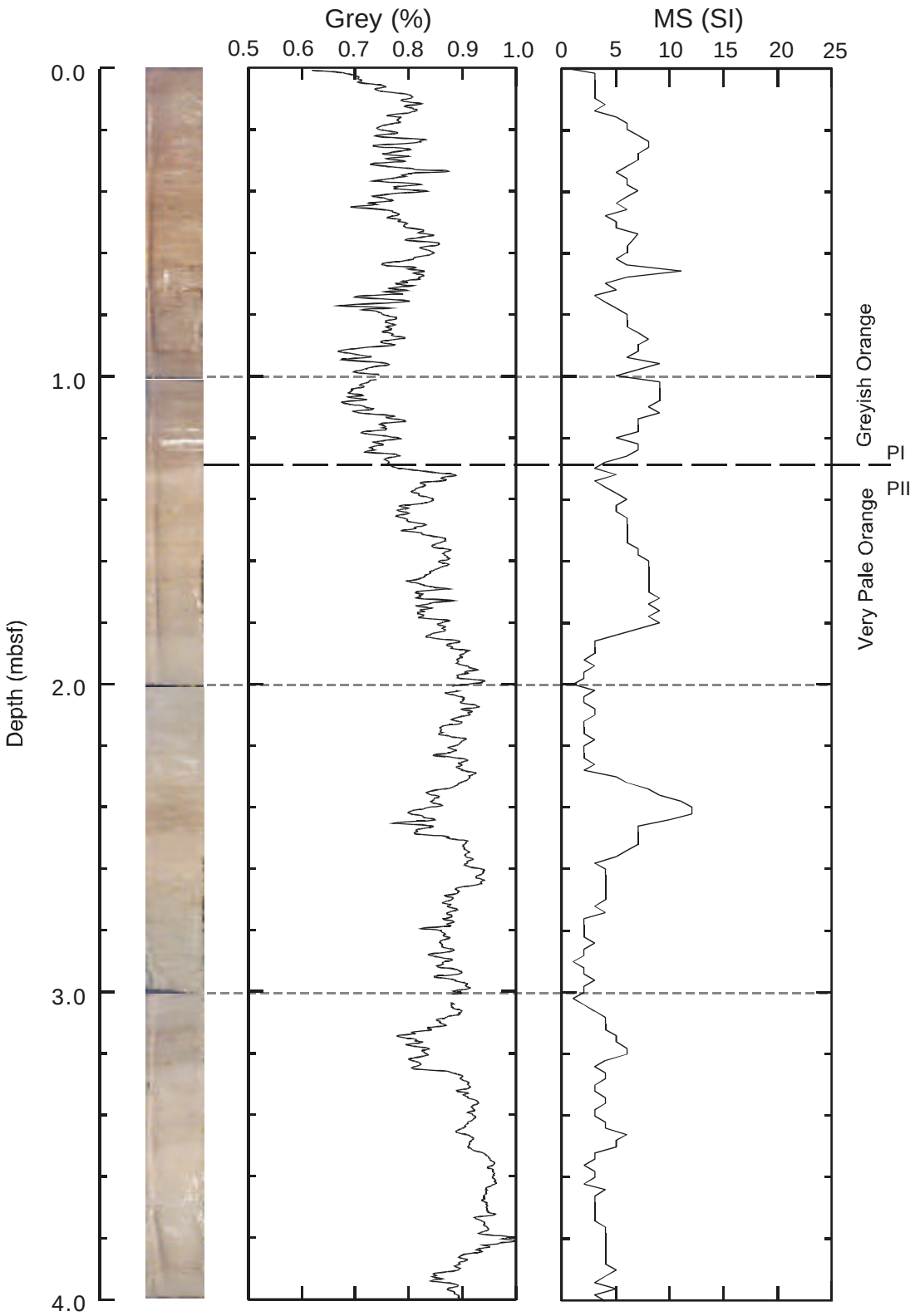

ZONÉCO 5
KG 13 (4.00 - 7.04 mbsf)